

Unmanned Aircraft System (UAS) Integration to Airspace and Collision Risk Assessment

by

© Bruno M. Artacho

A thesis submitted to the School of Graduate Studies
in partial fulfilment of the requirements for the degree of
Master of Engineering

Faculty of Engineering and Applied Science
Memorial University of Newfoundland

May 2018

Saint John's

Newfoundland and Labrador

Abstract

Near Mid-Air Collision (NMAC) risk is an impediment to the integration of Unmanned Aircraft System (UAS) into non-segregated airspace. It is quantified by a NMAC rate per flight hour, and this rate has been used for risk assessment for manned aviation. To estimate similar statistics with the inclusion of UAS in a known airspace, MIT Lincoln Laboratory (MIT/LL) has built an UAS-centric encounter model of the US National Airspace System (NAS). This thesis builds upon the MIT/LL encounter model to estimate a Canadian NMAC rate using on a standard proposed by National Research Council of Canada. The reported assessment takes into the account of the variation of field of view, radar range used for detection and tracking of the Intruder and the UAS achievable horizontal turn rate. Depending on the traffic, a notional radar-based detect-and-avoidance system could be demonstrated to have a lower NMAC rate than the Canadian NMAC rate.

Acknowledgments

I would like to thank my supervisor Dr. Siu O'Young for his help and support for my research and thesis. I extend the acknowledgement to my research colleagues at Memorial University of Newfoundland for their contributions during this work. I also would like to show my appreciation to Heidi Allen for her help in the preparation of this thesis.

The support of my parents Mauricio and Cristina and my sister Carolina, not only during the work for this thesis, but also during my entire academic studies and work.

Table of Contents

Abstract.....	ii
Acknowledgments.....	iii
Table of Contents.....	iv
List of Figures.....	v
List of Abbreviations and Symbols.....	vii
Chapter 1 Introduction.....	1
1.1 Problem Statement.....	2
1.2 Contributions.....	3
1.3 Organization.....	4
Chapter 2 Background.....	6
2.1 UAS Integration into the Airspace.....	6
2.2 Risk Assessment Definitions and Methods.....	9
Chapter 3 Collision Avoidance Threshold Determination.....	16
3.1 Well Clear Definition.....	17
3.2 CAT and NMAC Definition and Determination.....	19
Chapter 4 Encounter Model.....	29
4.1 Traffic Implementation and Simulation.....	35
Chapter 5 Collision Risk Analysis.....	44
5.1 Canadian Arctic Surveillance Application.....	66
Chapter 6 Conclusion.....	68
6.1 Future Work.....	69

List of Figures

Figure 1: System Fault Tree.....	11
Figure 2: Intruder bearing angle distribution [18]	14
Figure 3: Layered model for UAS [19].....	16
Figure 4: Detect and avoid procedure for the UAS [25].....	20
Figure 5: Distribution of acceleration observed in NAS by MIT/LL [27]	21
Figure 6: Initial simulation for CAT determination.....	22
Figure 7: Intruder with reduced initial distance	23
Figure 8: UAS and Intruder with unavoidable distance.....	23
Figure 9: Distance (nm) to avoid collision for all bearing angles and different velocities.....	25
Figure 10: Time (s) for collision avoidance for all bearing angles and different velocities.....	27
Figure 11: Acquired data in flight hours for the encounter model in NAS [27].....	30
Figure 12: Initial State Bayesian Network for the UEM [27].....	32
Figure 13: Transition State Bayesian Network for the UEM [27].....	32
Figure 14: Intruder in collision trajectory bearing angle	36
Figure 15: State and risk for the simulation [33]	39
Figure 16: NMAC contours for different distances and bearing angles [33]	40
Figure 17: NMAC probabilities for different times to approach (τ) [33]	41
Figure 18: MRS for different values of turn rate [31]	42
Figure 19: PRS examples in a three-dimensional case [31]	43

Figure 20: Aircraft density over the NAS in aircrafts/nm [27].....	46
Figure 21: Aircraft density over the NAS in aircrafts/nm between 10,000 ft. and FL180 [27] ...	47
Figure 22: Intruder bearing angle distribution	48
Figure 23: Avoidance maneuvering performed by the UAS	51
Figure 24: NMAC distribution for different radar ranges with ± 120 detection.	52
Figure 25: NMAC reduction for different radar ranges with ± 120 detection.....	53
Figure 25: NMAC distribution for Intruders with 360° detection.	54
Figure 26: NMAC reduction for different radar ranges with detection of all bearing angles.	55
Figure 27: Distribution of velocities observed in NAS uncontrolled airspace [27]	57
Figure 28: NMAC probability distribution for Intruders limited to 170 kt.	58
Figure 29: NMAC reduction with $\pm 120^\circ$ detection and velocity limited to 170 kt.	59
Figure 30: NMAC distribution for Intruders limited to 170 kt. with 360° detection.	60
Figure 31: NMAC reduction with 360° detection and velocity limited to 170 kt.	61
Figure 32: NMAC reduction with 360° detection and velocity limited to 170 kt. under 5,000ft.	63
Figure 33: NMAC rates for different densities	64
Figure 34: NMAC rates for detection angles, ranges and locations in Canada	65

List of Abbreviations and Symbols

ATC	Air Traffic Control
ATM	Air Traffic Management
BVLOS	Beyond Visual Line of Sight
CAA	Civil Aviation Authority
CASA	Civil Aviation Safety Authority
CAT	Collision Avoidance Threshold
CPA	Closest Point of Approach
DAA	Detect and Avoid
DMOD	Distance Modification
DOD	Departments of Defense
DHS	Departments of Homeland Security
ETA	Event Tree Analysis
FTA	Fault Tree Analysis
GA	General Aviation
HMD	Horizontal Miss Distance

<i>HMD</i>_{WC}*	Horizontal Separation Threshold
ICAO	International Civil Aviation Organization
IFR	Instrument Flight Rules
LL	Lincoln Laboratory
MA	Manned Aircraft
MAC	Mid-Air Collision
MALE	Medium Altitude Long Endurance
MIT	Massachusetts Institute of Technology
NAS	National Airspace System
NMAC	Near Mid-Air Collision
NRC	National Research Council
R&D	Research and Development
RPA	Remotely Piloted Aircraft
RPAS	Remoted Piloted Aircraft System
RTCA	Radio Technical Commission for Aeronautics
TC	Transport Canada
TSB	Transportation Safety Board

UAS	Unmanned Aircraft Systems
UAV	Unmanned Aircraft Vehicle
UEM	Uncorrelated Encounter Model
VFR	Visual Flight Rules
VMD	Vertical Miss Distance
VMD_{WC}^*	Vertical Separation Threshold
WC	Well Clear
WCV	Well Clear Violation

Chapter 1

Introduction

Since early aviation developments, in the 1950s, Detect and Avoid (DAA) systems have been a relevant and necessary aspect for improvements. Its importance for research purposes started to intensify during the 1960s with the frequency increase of North Atlantic flights. As a consequence, the safety concern related to a possible collision started to be one of the top research priorities.

Near mid-air collision (NMAC) risk is an impediment to the integration of unmanned aircraft system (UAS) in non-segregated airspace. NMAC risk can be quantified by the NMAC rate per flight hour, and this has been used for risk assessment for manned aviation. For example, the Canadian national NMAC rate for General Aviation (GA) traffic is estimated to be $7.14 \cdot 10^{-7}$ for 2015.

To assess statistical NMAC risk for the addition of UAS in a known airspace, MIT Lincoln Laboratory (MIT/LL) has built an UAS-centric encounter model of the US National Airspace System (NAS) based on collected radar tracks of relevant air traffic. This model was used to analyze statistical NMAC rates for different radar detection distances and field of view in air traffic densities covering different regions of the USA and Canada.

The proposed avoidance standard recommends maintaining a separation distance of no less than $(2\tau + 15) \times v$ or 1 nm, where τ is the maneuver time (in seconds) to avoid a NMAC and v is the closure rate between the UAS and an Intruder aircraft.

The assessment considers the variation of field of view and range of a radar used for detection and tracking of the Intruder, the achievable horizontal turn rate of the UAS, air traffic density and pattern of the airspace in which the UAS operates.

Since NMAC rates vary with the airspace density, it is possible that the UAS operation meets the safety standards without Sense and Avoid capabilities for some regions, whilst other regions require it with a minimum radar range.

The proposed methodology has been simulated in different scenarios for risk estimation to allow cost benefit analysis of different radar specifications.

1.1 Problem Statement

Differently than the US, Canada currently does not possess a tool for assessing the risk of implementation of UAS into its airspace. It is desired to develop, including concepts and methodologies well accepted and implemented in other countries, an application that allows the assessment of risk when incorporating UAS in the Canadian airspace, as well as to determine the Minimum Operational Performance Standards (MOPS) for its operation.

This thesis builds upon the MIT/LL encounter model to estimate a Canadian NMAC rate using an avoidance standard proposed by the National Research Council of Canada (NRC). The objective is to develop a methodology to quantify safety of Beyond Visual Line of Sight (BVLOS) UAS operations by estimating the frequency of an UAS in a potential NMAC trajectory with a manned aircraft (MA), where the UAS is assumed to have certain given sensor and maneuver capabilities for the DAA of the MA.

The methodology developed should be able to assess levels of safety for operation in different environments, determining the requirements for UAS operations in each specific application desired.

The objectives of this thesis are:

- Create a new methodology to assess the risk of NMAC rate, and consequently the risk of flying UAS in different aircraft densities
- Quantify the safety of Beyond Visual Line of Sight (BVLOS) operations of UAS.
- Identity MOPS for radars when implementing collision avoidance, following proposed recommendations for the Canadian Airspace.

1.2 Contributions

The expected contributions in the development of the Risk Assessment tool is to determine a NMAC rate estimation method considering the air traffic density of the target area, aircraft and radar specifications.

The creative combination of a risk model, an air traffic/density model, and a characterization of the sensor and aircraft performances allows the computation of NMAC risk, which is a function of traffic density and DAA capabilities. The quantification of this trade-off is necessary for the establishment of MOPS needed both for the regulators to safeguard air safety, and for the manufacturers to build compliant DAA equipment.

When there are significant differences in traffic densities within a national or an international airspace system; e.g., between urban and the Arctic regions of Canada, the MOPS [1] for the radar is different. This offers a venue for the “baby-step” approach in the validation of prototype DAA equipment in sparse air density area under case-by-case exemptions or under the Special Flight Operations Certificates (SFOC) system in Canada.

The implementation of the method permits the analysis of the required radar range and field of view to the specific UAS operation, contributing for the NMAC and consequently accident rate reduction whilst adopting adequate equipment with the cost/risk analysis of its implementation.

The developed application determines the safety levels of operation for different airspace traffic densities that the UAS operates, determining the required notional radar-based Detect and Avoid (DAA) system range and field of view required in order to achieve a NMAC rate lower than the Canadian National $7.14 \cdot 10^{-7}$ NMAC/h reference rate.

1.3 Organization

This thesis is organized as follows:

- Chapter 2 presents a background and literature review of UAS operations into the different airspaces, including procedures proposed and applied by regional air space regulatory agencies, as well as Risk Assessment methods implemented to its operation and tests.
- Chapter 3 describes the C-based method developed for the calculation of the minimum time and distance required in order to the last-ditch avoidance maneuver be performed by the UAS to avoid Intruders in direct collision route. It describes the requirements,

regulations and dynamics used in the development of the software that is essential to calculate the minimum distance required for the radar detection posteriorly utilized to assess NMAC risks, according to standards proposed by NRC for the Canadian airspace.

- In Chapter 4, the encounter model utilized to determine the NMAC rate in this analysis is described. It presents the operation of the model developed from MIT/LL encounter model adapted for the Canadian airspace. The parameters adopted, and the method used to assess the NMAC rates are described. It also presents an analysis and preview of a real world implementation of the method in the Canadian Arctic, as part as a project developed by request of Transport Canada.
- Chapter 5 includes the implementation and analysis of the developed methodology for the NMAC rate determination, as well as the calculation of required radar ranges for UAS flying in different air traffic densities to meet and surpass levels of safety currently observed in manned aviation.
- Chapter 6 presents the conclusions from the Risk Assessment method developed and implemented for Canada, including the expected contributions and future work.

Chapter 2

Background

2.1 UAS Integration into the Airspace

Establishing the context is essential to define the project scope. The integration of UAS into the airspace shares the same common concept: first, the real necessity of implementing UAS in the non-segregated airspace with its involved risks; secondly, to establish regulations in order to avoid undesired hazards.

The International Civil Aviation Organization (ICAO) establishes bases for subsequent regulations at Circular 328, “Unmanned Aircraft Systems (UAS)” [2] in which, in the most recent edition, it specifies as the main goal for aviation regulatory contributions as obtaining and maintaining the highest possible and uniform level of safety. It also states that when considering UAS, the goal is considered to be maintaining and ensuring the current level of safety, including other aircraft and safety of persons and properties on the ground.

Federal Aviation Administration (FAA) includes the UAS integration in the National Airspace (NAS) as part of its recent publications [3] and highlights the considerations to be taken into future regulations as for example, the non-damaging interaction of UAS with the already existent elements in the airspace:

Ultimately, UAS must be integrated into the NAS without reducing existing capacity, decreasing safety, negatively impacting current operators, or increasing the risk to airspace users or persons and property on the ground any more than the integration of comparable new and novel technologies.

Also, countries have been engaged to develop regulatory measurements that allow a certain level of safety in the airspace. For example, Civil Aviation Safety Authority (CASA) has an ongoing project which will introduce a regulation and guideline to industry in the operation of UAS in the Australian Airspace [4]. In more recent years, academic studies were conducted in order to determine risk analysis of flying UAS over inhabited areas in Australia [5]. It is important to point out that, for the scope of this project, the focus relies on air hazards.

The level of safety is also mentioned by EUROCONTROL in its latest document related to UAS, in this case referenced as Remotely Piloted Aircrafts (RPA) [6]:

Firstly, RPA operations should not increase the risk to other airspace users; secondly, ATM procedures should mirror those applicable to manned aircraft; and, thirdly, the provision of air traffic services to RPAs should be transparent to ATC controllers. The specifications are also innovative insofar as they are not constrained by limitations in current RPA capability such as sense-and-avoid. The specifications will therefore only be practicable once Industry develops this and other necessary technology.

The UAS integration with the European Airspace was successfully conducted in the German Air Traffic Control (ATC), as described in [7]. During the operations at the German Air Space the use of hardware applications that increased safety levels is relevant, such as Traffic Collision Avoidance System (TCAS) and lighting/markings on the aircraft, as well as the complete immersion of UAS into the ATC. Complementary to this work, the experiment was conducted in a denser air space with air traffic control.

UAS Roadmaps in Australia are currently being developed. As pointed by [8], it has goals to integrate military, civil and industrial development users, with priorities including: Securing

communication and information; Ensure safety of Airspace operations; Autonomy of Unmanned Vehicles. The proposal takes into consideration payloads (hardware) and human factors for its analysis of risk from implementation of UAS into the airspace system.

As a result of regulations, UAS are restricted to be flown within the human pilot visual range of sight, which creates a difficulty on its larger implementation. Some techniques are currently being developed in order to widen options of flying beyond the line of sight as mentioned by Civil Aviation Authority (CAA) in Cap 722 [9]:

An approved method of aerial collision avoidance is required thus UAS operations will not be permitted in non-segregated airspace, outside the direct unaided visual line-of-sight of the pilot, without an acceptable Detect and Avoid system.

Hence, industry is widely developing systems required to achieve the acceptance level determined by the corresponding administration and, specifically for Canada, Transport Canada (TC).

The thesis focuses on the probability calculation of the separation loss between UAS and MA. The analysis of levels of safety and collision rates of UAS operations in different regions in the USA and Canada are performed. The thesis also determines the required ranges for radar in order to detect Intruder aircraft and successfully perform avoidance maneuvering, as well as safety improvements from the detect and avoid incorporation.

As for the scope of this project, applications from the Uncorrelated Encounter Model (UEM) developed by MIT/LL will be refined in order to simulate an UAS flying over an uncontrolled airspace in Canada.

2.2 Risk Assessment Definitions and Methods

Given the regulatory entities directives, it is noticeable that UAS integration in the airspace has associated risks. Consequently, it is necessary to perform a risk assessment in order to successfully develop a DAA method that permits the UAS implementation in the airspace, without the requirement of a ground pilot.

The evaluation of safety levels in aviation is performed by the analysis of different metrics, such as the Mid-Air Collision (MAC) and NMAC rates. The risk assessment of the UAS introduction into the airspace can be successfully evaluated by the determination of those metrics with the incorporation of UAS. The MAC and NMAC rates provide essential insight of the safety associated with air traffic operations.

Both MAC and NMAC rates have been progressively decreasing over the past decades worldwide. This fact is credited to modernization of radars and systems adopted for ATC. For the Canadian airspace, the Transportation Safety Board of Canada (TSB) periodically publishes statistics and analysis considering accidents and collisions. MAC and NMAC rates can be, therefore, estimated from reported statistics. For the scope of this project, NMAC is utilized since it defines the volume for collision constantly for every aircraft, making it possible to analyze a general risk associated with the operation of several UAS and aircraft models without the size and application of the aircraft (UAS and Intruder) affecting the simulation. It also decreases the complexity of the simulation, resulting in a performance improvement for the analysis.

As a guideline for the development of risk assessment methods in UAS, [10] presents steps that lead to the system development and evaluation. The risk identification stage establishes origin

and cause for failures. In the analysis stage, each scenario is examined in nature, being compared and evaluated with the safety criteria.

In this work, the analysis is described in the following sections: Method to identify NMAC causes (present, and Chapter 3); encounter simulated model (Chapter 4), including probabilistic methods used to determine the level of safety from the simulated scenarios.

There are several established techniques [11] for risk identification:

- Event Tree Analysis (ETA) pertains to isolating a hazard in order to evaluate the outcome of sequential failures. In other words, it logically models the scenario by analyzing the success or failure in a singular initial trigger event, following paths according to probabilities and outcomes. In [12], this technique is used to describe the fatalities upon certain conditions.
- Fault Tree Analysis (FTA) combines events that lead to a hazard. It is often applied combined with ETA, as seen in [13], aiming to simulate incursions on airports runways.
- TOPAZ analyzes the scenario combined with Monte Carlo Simulation technique (computational method for repeated random sampling data from a database, in order to perform a numerical analysis. The steps for its assessment consist of: Definition of objective, operations, hazards and their combinations; and construction of its scenarios in order to identify its severities, frequency of occurrence and tolerability.

Collisions with Intruders are considered a greater concern regarding UAS flight safety due to elevated potential hazard to the UAS and the Intruder aircraft. As defined in [14], the probability of collision is a direct relation between the probabilities of UAS fail, loss of separation, encounter and the Intruder being unable to detect the UAS. FTA, in combination with Monte Carlo

Simulation, has been chosen to determine the NMAC rate and levels of safety during operations. Figure 1 presents a high-level Fault Tree for the system.

Since the detection range is dependent on the geometry of the converging trajectory, the function between the probabilities is only notional, meaning that the NMAC rate cannot be calculated as the product of probabilities for the DAA failure and the converging track. Hence, Monte Carlo simulation for each track is needed to assess the specific DAA case. It is assumed that the rate of the converging track can be scaled by the airspace density. The “AND” at this level is valid.

The dependency between factors, described and demonstrated in Figure 1, is critical for the adoption of the Encounter Model using Markov’s model for the system simulation.

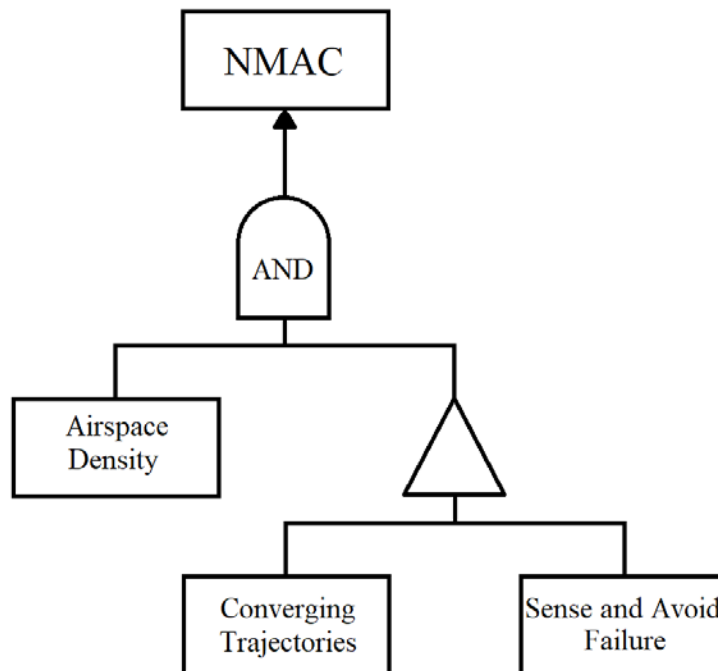


Figure 1: System Fault Tree

In the system developed, Intruders are positioned using Monte Carlo Simulation. The calculation of the final NMAC rate is estimated using the Fault Tree from Figure 1 and adopting probability values determined in the following sessions.

UAS were initially developed to be a safer alternative for MA, eliminating possible errors caused by human pilots. Consequently, the introduction of UAS should fulfill the requirement of maintaining or decreasing the accident frequency in the airspace. Risk analysis for UAS include: Potential damage to other aircrafts and hazard for population and constructions on the ground.

The probabilistic estimation of an UAS ground impact model is calculated and specified in [15]. The approach basis is defined by the modelling of the ground impact of a UAS, and by the sequential events represented in the event tree.

The event tree is used to represent different possible outcomes as a consequence of certain events [15]. In this case UAS is referred by UAV:

The event-based model first describes whether a failure of the UAV system has occurred. If it has, then an accident has occurred that will result in an uncontrolled ground impact.

Alternatively, [16] defines a three-step approach in order to address the risk:

- Identification of the risks impacting the implementation of the roadmap Research & Development (R&D) on Remoted Piloted Aircraft System (RPAS).
- Characterization of risks according to their causality and their criticality.
- Define a list of mitigating actions aimed at preventing the risks to occur.

Risks are categorized as internal, from implementation and external, proposing an adequate mitigation action for each predicted situation.

It is important to notice that despite accounting for mitigation effects, the model for risk estimation has assumptions to simplify its determination, consequently imposing limits for its possible applications. For instance, the model described in [15] does not consider demographic density variation, whilst [17] determines density by published census data.

Collisions with Intruders are considered a greater concern regarding UAS flight safety due to its elevated potential hazard to the UAS and the Intruder aircraft. As defined in [14], the probability of collision is a direct relation between the probabilities of UAS fail, loss of separation, encounter and the Intruder being unable to detect the UAS.

It is relevant to observe that the probabilities of failure described above are not independent. Therefore, the implementation of simulation (MIT/LL UEM) is useful for the assessment.

When accounting for risk, as pointed out by [18], bearing angle of the Intruder is an essential aspect to be observed. It allows effort to be focused on detecting and avoiding collisions. Figure 2 represents the distribution of Intruders from data simulation [18]. It is noticeable that this research simulation with MIT LL model obtained most of the occurrences in front of the aircraft, as expected by its forward velocity.

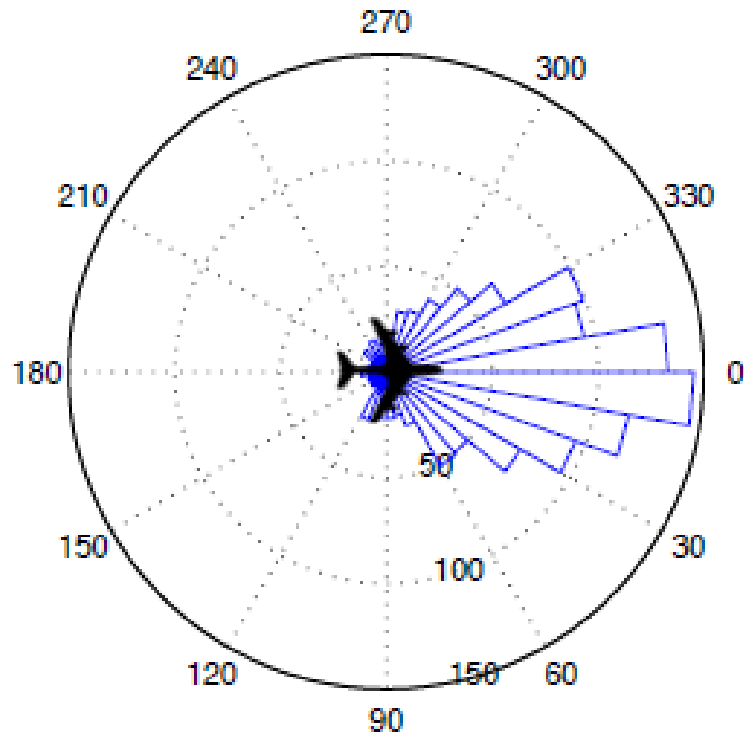


Figure 2: Intruder bearing angle distribution [18]

Considering the possible risks associated with the implementation of UAS, it is important to perform research and computational simulation in order to ensure that the operation of UAS in the airspace does not promote a negative impact in the current collision rate.

Currently available developments, including data analysis over NAS make it possible to adapt and implement collision risk analysis in different scenarios and applications, with possession of data analysis of the airspace, ground density and terrain.

Other developments and application experience were successfully completed in Germany, flying over controlled and denser airspace [7]. The use of these studies should be considered in order to diversify and increase strength of analysis in a different environment, as the Canadian Airspace.

As a result of the Monte Carlo simulation, it is possible to estimate the Risk Ratio of flying an UAS, considering possible fault sources and consequences in order to ensure that the operation will fulfill FAA, TC and ICAO directives.

It is concluded by this investigation that in order to obtain complete analysis and conclusions, it is recommended to adapt and integrate the MIT/LL model to perform simulation, since it uses a reliable and effective model, vastly used over industry and academia in a closer geographic region.

Chapter 3

Collision Avoidance Threshold Determination

Chapter 3 will present the methodology to determine the CAT required for the UAS to avoid an Intruder aircraft as a last-ditch effort. The software developed and simulation will follow recommendations proposed from NRC.

In order to standardize aircraft for simulation, a NMAC cylinder is defined to generalize aircraft of different shapes and sizes as a common volume, decreasing the complexity required for simulation. The NMAC volume consists of a cylinder with a radius of 500 ft. and a height of 100 ft.

Figure 3 demonstrates the common definitions of NMAC, Collision Avoidance Threshold (CAT), and Well Clear Violation (WCV). The definitions for Well Clear (WC) and CAT are defined by distinct methods. For the scope of this thesis, CAT and NMAC will be adopted for simulation and calculation.

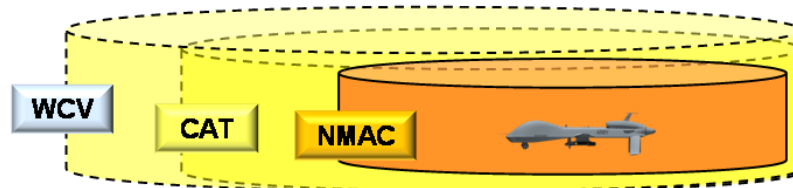


Figure 3: Layered model for UAS [19]

3.1 Well Clear Definition

Although not used in the scope of this thesis, it is important to clearly define the WC, since whilst its definition diverges from the one adopted, both definitions make use of a calculated term τ . Following the method described in [20], the WC is defined as the minimum distance between aircraft required to maintain certain levels of safety. Some variables need to be determined in order to calculate the WC values. Initially, the range, that is the distance between aircraft, is defined as:

$$r = \sqrt{x^2 + y^2} \quad (1)$$

With x and y being the distances from the latitude and longitude coordinates, respectively, between aircraft. From deriving Equation (1), the horizontal range rate is determined:

$$\dot{r} = \frac{dr}{dt} = \frac{x \cdot v_x + y \cdot v_y}{r} \quad (2)$$

Used on Equation (2), v_x and v_y represent the velocities for the x and y coordinates, respectively. With the values of range and range rate determined, the variable τ_{WC} is obtained [21]:

$$\tau_{WC} = -\frac{r}{\dot{r}} \quad (3)$$

It is important to point out, that Equation (3) can only be applied on the condition that the range rate is different than zero. An additional modified distance is required for the calculation of the WC range, τ_{mod} . Its calculation takes into account a constant distance modification (DMOD), defined as the alert threshold distance (i.e. 4,000 ft.), [21] and [22].

$$\tau_{mod} = -\frac{r - \left(\frac{DMOD^2}{r}\right)}{\dot{r}} = -\frac{r^2 - (DMOD^2)}{r \cdot \dot{r}} \quad (4)$$

Equation (4), $DMOD^2/r$ includes a range buffer, dependent of DMOD and the horizontal range. The next function which must be determined is the horizontal range as a function of time, [23]:

$$r(t) = \sqrt{(x_0 + v_x \cdot t)^2 + (y_0 + v_y \cdot t)^2} \quad (5)$$

Where x_0 and y_0 are the initial distances between aircraft. The time for the minimum distance is determined when the derivative of Equation (5) is zero. Therefore, the time to the closest point of approach (CPA) is obtained by:

$$t_{CPA} = \max\left(0, -\frac{x_0 \cdot v_x + y_0 \cdot v_y}{v_x^2 + v_y^2}\right) \quad (6)$$

Combining Equations (5) and (6), the horizontal miss distance to CPA (HMD) is determined as [23]:

$$HMD = \sqrt{(x + v_x \cdot t_{CPA})^2 + (y + v_y \cdot t_{CPA})^2} \quad (7)$$

With a similar method, the Vertical Miss Distance (VMD) is calculated:

$$VMD = h + v_h \cdot t_{CPA} \quad (8)$$

Where h is the vertical distance between aircraft and v_h is the vertical rate. With all values determined, the condition on which the Intruder is considered within the WC can be defined as [23]:

$$[0 \leq \tau_{mod} \leq \tau_{mod_{WC}}^*] \text{ and } [HMD \leq HMD_{WC}^*] \text{ and } [V_s \leq VMD_{WC}^*] \quad (9)$$

Where τ_{mod} is the range τ modified and V_s is the absolute vertical distance, the Horizontal Separation Threshold is HMD_{WC}^* , and the Vertical Separation Threshold is VMD_{WC}^* .

3.2 CAT and NMAC Definition and Determination

In the simulation the Intruder aircraft will fly within an Encounter Cylinder, as determined by both the radar specifications calculated, software limitations and also optimized for NMAC occurrences analysis.

NRC defines the best practice standard, for the detection and avoidance distance required to perform a maneuver within acceptable safety levels to be equivalent to $2\tau + 15$ seconds or at least 1 nm [24], where τ is the minimum time required to perform a successful avoidance maneuver.

In order to perform avoidance maneuvers, the UAS follows the procedure described in Figure 4. In the initial $\tau + 15$ seconds, the UAS detects and declares a valid track and threat, determines the action and commands. Finally, in the remaining τ seconds, the last-ditch maneuver is executed to avoid the Intruder aircraft.

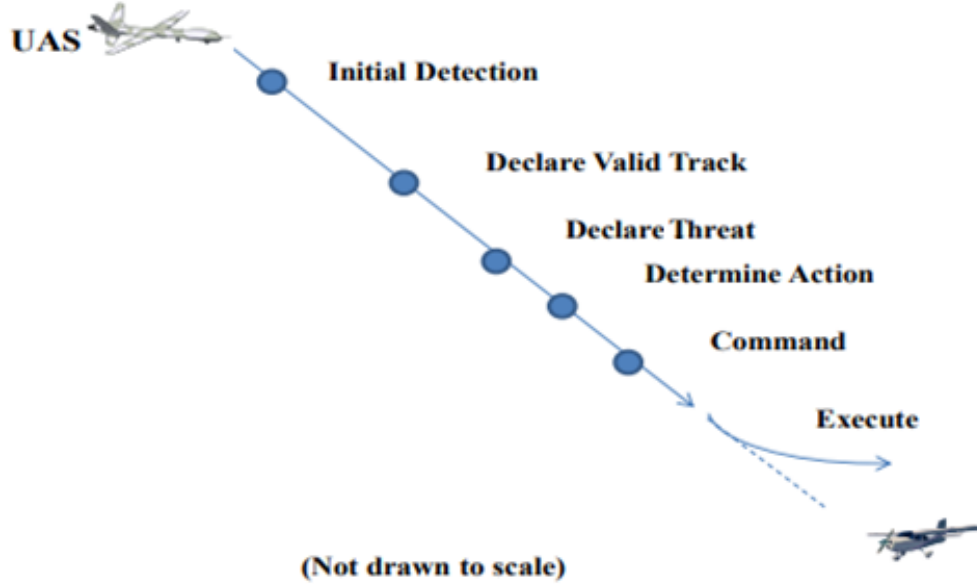


Figure 4: Detect and avoid procedure for the UAS [25]

It is assumed that large values calculated for the avoidance procedure are not threats and, therefore, do not pose a potential collision scenario.

In order to obtain the minimum time and distance for avoidance maneuvering, a C-based software was developed, following recommendations by [24].

The value of the CAT is defined by [26] as:

$$\forall x_{\text{Int.}}(\tau), \exists m \in u_{\text{UA}}^{\text{CA}} \text{ such that } \overline{NM\overline{AC}} \quad (10)$$

Where $x_{\text{Int.}}$ is defined as the states for the Intruder (position in coordinates x and y , and its constant velocity). $u_{\text{UA}}^{\text{CA}}$ is the set of all possible moves for collision avoidance.

Encounter simulations are performed to determine the distance and time for CAT. The simulation consists of tracking trajectories for both UAS and Intruder in a co-altitude leveled flight.

Each aircraft is controlled by the variables $[x, y, v, \psi, \dot{\psi}]$, that represent longitude, latitude, velocity, heading angle, and turn rate, respectively.

Since the goal is to determine the minimum threshold required for a last-ditch avoidance maneuver, the worst-case scenario is adopted for simulation. That is, the Intruder heading will result in a direct collision route. The value is calculated for each specific scenario, taking into consideration the Intruder bearing angle and the velocities for both the UAS and the Intruder.

Therefore, the Intruder turn rate is selected as 0G in order to calculate the minimum required distance for avoidance maneuvering (τ), with the UAS maneuver being performed as last-ditch. Also, since the simulations are within a small period of time ($t < 20$ s), the velocities are considered to be constant. From the analysis of the flight data acquired from NAS for the development of the encounter model by MIT/LL for acceleration in Figure 5. It is confirmed that the constant velocity assumption to determine CAT is correct for most Intruders in the data in which the observed acceleration is zero or small for most cases, and especially for short duration simulation.

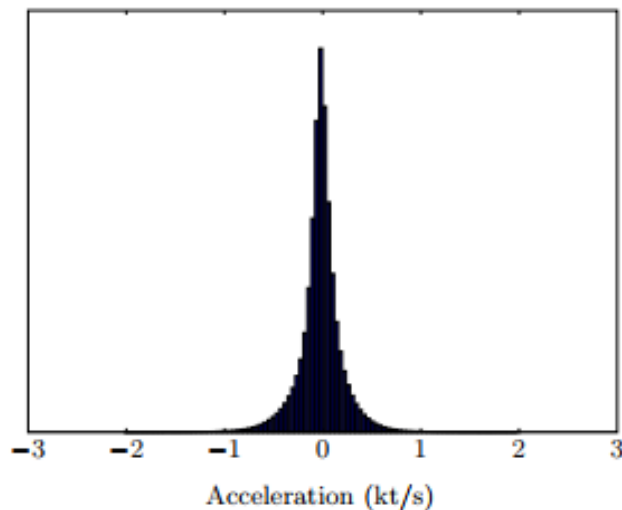


Figure 5: Distribution of acceleration observed in NAS by MIT/LL [27]

In a specific bearing angle scenario between the UAS and the Intruder, an initial distance between aircraft is selected. The UAS detects the Intruder and calculates the possible avoidance maneuvers, considering all possible headings for avoidance. Figure 6 demonstrates the first simulation performed in order to determine the CAT for one particular bearing angle.

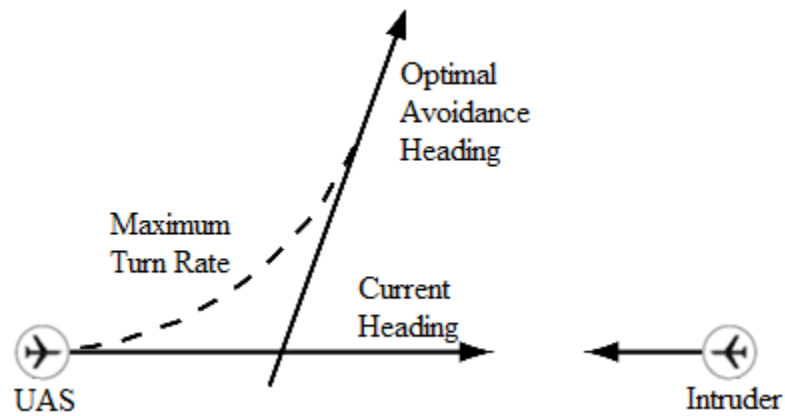


Figure 6: Initial simulation for CAT determination

Following the initial distance where there is at least one possible avoidance heading for the UAS, the Intruder is positioned at a closer initial distance from the previous iteration, and the potential collision scenario is simulated for another iteration, as shown in Figure 7.

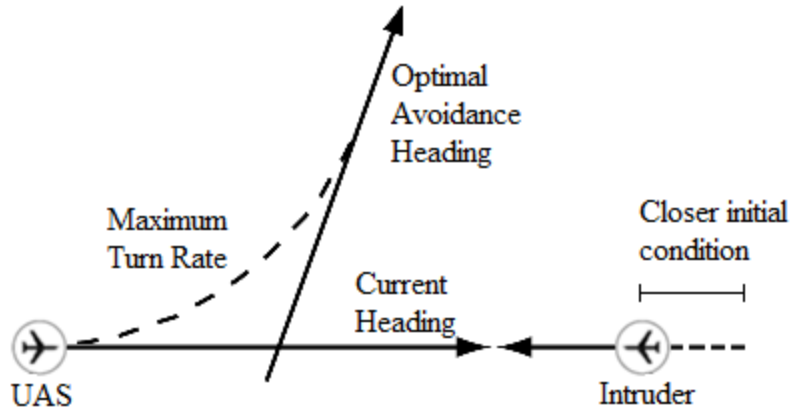


Figure 7: Intruder with reduced initial distance

This procedure is repeated until it reaches a scenario where there are no possible avoidance maneuvers for the UAS to perform with an Intruder approaching from that determined bearing angle and distance between aircraft. The scenario described is illustrated in Figure 8. In this case, the last simulated distance, where at least one avoidance maneuver was still possible, is determined as the CAT for that particular Intruder.

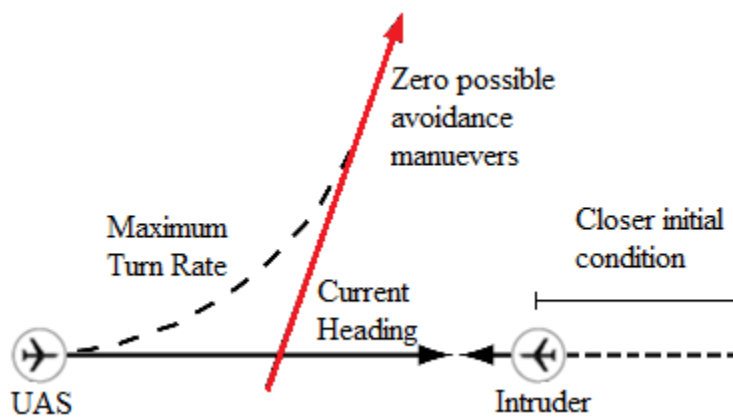


Figure 8: UAS and Intruder with unavoidable distance

The following simulations to determine NMAC rate are performed considering both the Intruder velocity and the heading angle throughout the flight.

Each iteration of the simulation consists of:

- The UAS is initialized at the origin, flying with a constant velocity and heading north (0°). The Intruder is positioned at an initial distance and bearing angle selected.
- Avoidance maneuvers are successively selected according to the heading angle resolution. For each final heading angle of the maneuver, it is recorded whether or not a NMAC occurs, determining if the avoidance was successful.
- In case of at least one successful avoidance, both aircraft are reinitialized with the Intruder's relative distance reduced, repeating the procedure. If there is no possible maneuver to avoid a NMAC, the previous distance simulated is determined to be the CAT for that specific pair of velocities and bearing angle.

The simulation described can be synthesized in the following algorithm, where V_{UAS} is the velocity of the UAS, $V_{INTRUDER}$ is the Intruder velocity, ψ is the avoidance heading angle, and β is the bearing angle between the aircraft.

Algorithm – Determine CAT

```

1: function Determine CAT( $V_{UAS}$ ,  $V_{INTRUDER}$ ,  $\beta$ )
2:   for  $\beta \in [0^\circ, 360^\circ]$  with  $1^\circ$  increment > do
3:     for  $r \in [0, 1000]$  with 30 ft. decrement > do
4:       while NMAC avoided do
5:         for  $\psi \in [0^\circ, 360^\circ]$  with  $1^\circ$  increment > do
6:           if UAS avoids NMAC then
7:             Record newer minimum distance for avoidance
8:           else
9:             Use last recorded minimum as CAT distance and time
10:          Exit while loop
11:        end for
12:      end while
13:    end for

```

```
14:   end for
15: end function
```

Algorithm 1: Algorithm for Collision Avoidance Threshold Determination

Conducting the simulation for different sets of velocities and bearing angles, and considering UAS velocities, the CAT contours are obtained, as shown in Figure 9: Velocity pairs for the UAS and Intruder are: (a) 50 kt. and 150 kt.; (b) 100 kt. and 150 kt.; and (c) 50 kt. and 100 kt..

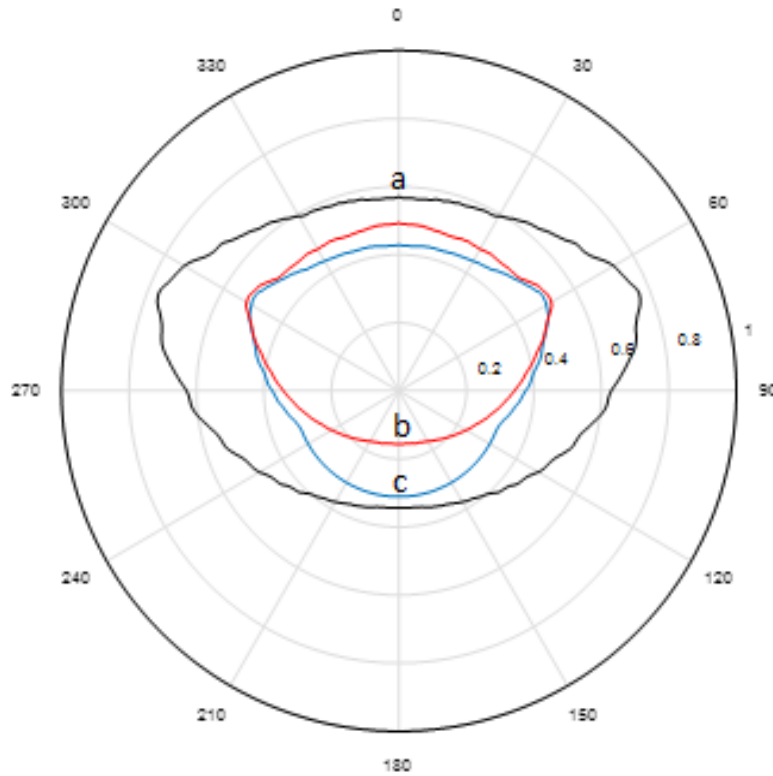


Figure 9: Distance (nm) to avoid collision for all bearing angles and different velocities

The simulations' definition parameters are: Distance resolution of 30 ft., time resolution of 1 second, and heading resolution of 1°.

It is observed that the required distance increases for lower velocities for the UAS (contours b and c), due to slower maneuvering speed to avoid the Intruder. In addition, bearing angles for side-on collisions (ranging from 60° to 90° , and its symmetrical pair between 270° and 300°), demand larger distances due to the critical approach angle of the Intruder, hindering avoidance maneuvering. This effect is accentuated when the UAS is flying with lower velocities relative to the Intruder.

As an example of required detection time, when the Intruder is flying at 100 kt. and the UAS at 50 kt. with a turn rate of 2G or $6^\circ/s$, and considering a radar acquisition time of 10 seconds, either 45 seconds or 1.88 nm is necessary in order to successfully fulfill the best practice values for a head-on collision, whilst either 55 seconds is required for tail-chase collision or 0.76 nm, therefore the adopted value is 1 nm.

Derived from the required distance, the software calculates the required time for last-ditch avoidance maneuvering (τ), considering the distance and relative velocity between aircraft in a direct collision route.

Figure 10 demonstrates the required times to avoid collisions from all bearing angles in the same sets of velocities for UAS and Intruder, distributed from the inner to outer contour in the same sequence: (a) 50 kt. and 150 kt.; (b) 100 kt. and 150 kt.; and (c) 50 kt. and 100 kt.. Analogously, a larger amount of time is required for bearing angles inside the range of 60° to 90° as well as between 270° and 300° . Lower UAS velocities demand more time to successfully avoid Intruders (contours a and b).

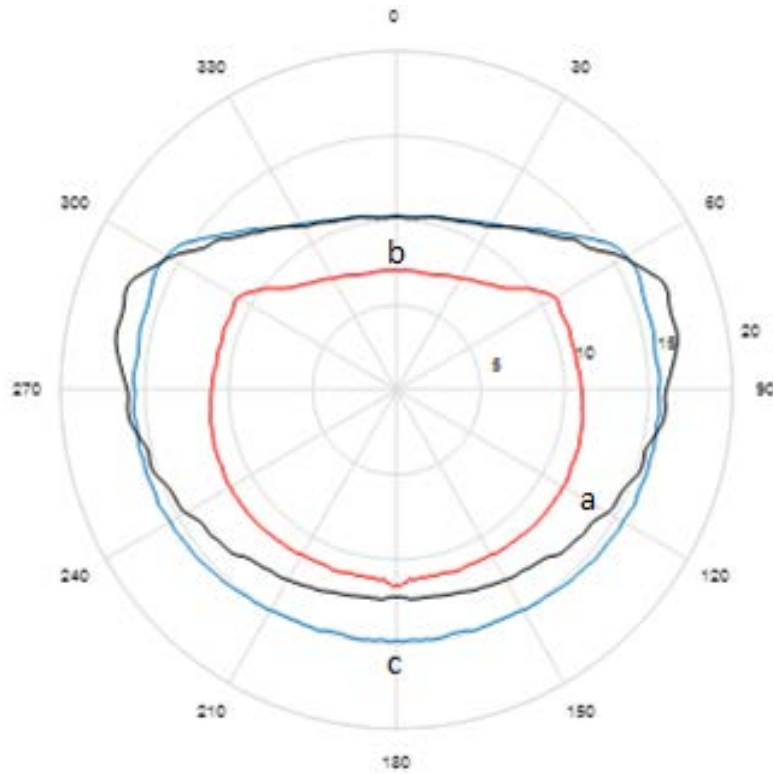


Figure 10: Time (s) for collision avoidance for all bearing angles and different velocities

Following the time calculation, the distance correspondent for $2\tau + 15$ seconds is calculated. This value is essential to determine radar range requirements. A simulation will be performed to determine the efficiency of different ranges of radar for the detection of Intruders when performing collision avoidance maneuvering according to the $2\tau + 15$ seconds' standard.

Also, the calculated values are used for the selection of an optimal Encounter Cylinder when executing Monte Carlo Simulation and the calculation of volume "swept" by the Encounter Cylinder during flight. Considering simulations for different velocities pairs it is observed that a radius of 3 nm and height of 200 ft is sufficient to fulfil the requirements for simulation of the Encounter Model within 60 seconds while maximizing the simulation time. Therefore, the

Encounter Cylinder is defined to have a radius of 2 nm and height of 200 ft for the model developed to the Canadian Airspace from MIT/LL UEM.

Chapter 4

Encounter Model

Chapter 4 will present a review of the MIT LL encounter model used as basis for the realization of this thesis. Further analysis and developments are conducted in order to allow the application of the encounter model for the Canadian Airspace and determine separation distances for safety improvements.

In order to simulate encounter situations, different statistical models were developed considering several applications, scenarios, and aircraft types.

Based on aircraft dynamics, regulatory agencies' standards for collisions and, in some cases, years of radar data analysis, aircraft simulation was developed and improved for aircraft encounters, generating essential data to estimate the risk of collision in a specific scenario.

The main function of an UEM [28], is to generate scenarios between the UAS and the Intruder aircraft with a potential for a hazardous event, based on observed real flight data.

The UEM was developed in 2006, by request of the FAA and US Departments of Defense (DoD) and Homeland Security (DHS) this new encounter model incorporates both MA and UAS by considering 130 radars and almost a year of data in the NAS. Figure 11 presents the radar data acquired to the MIT/LL model in flight hours divided into 1/6 of degree by 1/6 of degree cells.

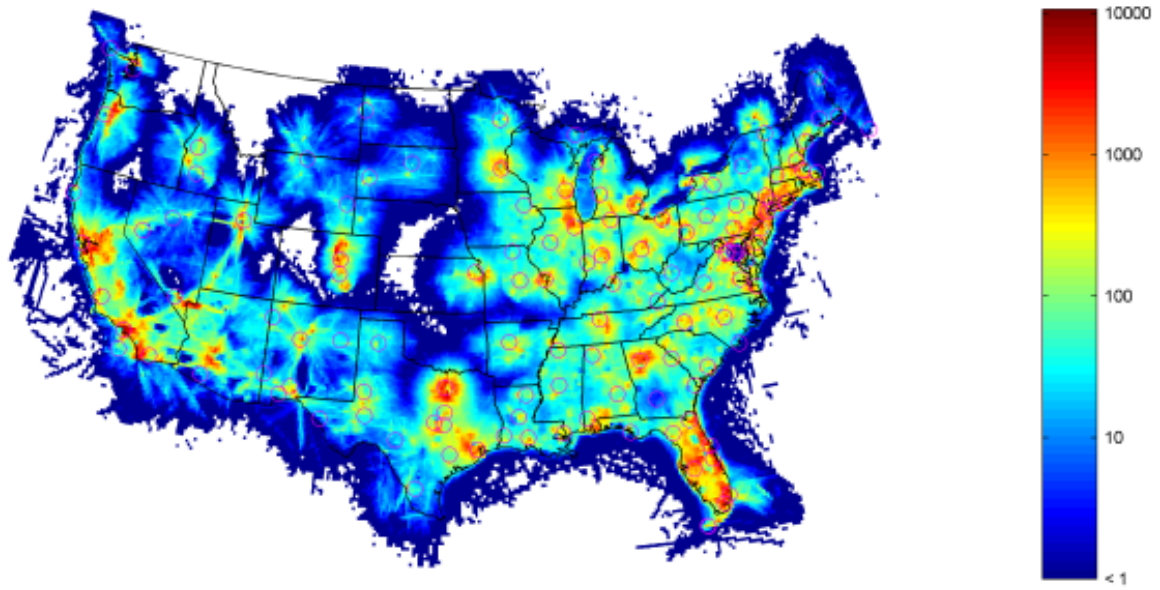


Figure 11: Acquired data in flight hours for the encounter model in NAS [27]

This model is currently adopted by the Radio Technical Commission for Aeronautics (RTCA-SC228) for its risk analysis and tests, and is, therefore, a method with proven acceptance and efficiency.

As presented in [29], this UEM takes into consideration altitude class and layer, airspeed, acceleration, turn rate, and vertical rate as variables for the model. With the initial state and transition dynamical model as a stochastic Markov model, tracks are created following aircraft tracks observed during actual flights through NAS.

Specifically, the MIT LL model simulates encounters including aircraft flying under Visual Flight Rules (VFR), where the MA do not see the UAS artificially inserted into the traffic pattern.

In the simulation, it is initially considered that both the UAS and the Intruder are flying without any detection and avoidance capability, that is, both aircraft are flying “blind”. Further

into the simulation, the UAS detection is included whilst the Intruder remains in “blind” flying conditions.

The UEM adopts Markov’s process, that consists of the determination of future probabilities by the most recent values. Specifically, for a stochastic process, a function is a Markov process if, for every term in time, Equation (11) is equivalent to Equation (12) [30]:

$$P(x(t_n) \leq x_n | x(t_{n-1}), \dots, x(t_1)) = P(x(t_n) \leq x_n | x(t_{n-1})) \quad (11)$$

$$P(x(t_n) \leq x_n | x(t) \text{ for all } x(t_1)) = P(x(t_n) \leq x_n | x(t_{n-1})) \quad (12)$$

For the UEM, the Markov’s model is defined as how the state of a system changes for a certain period where the assumption of the future probability in a future state is defined exclusively by the current state [28]. The model also enables the capability for collision avoidance algorithms implementation. The UEM applies Markov’s processes since allows testing for present and future collision avoidance algorithms, in a realistic and rigid manner, as a consequence of the fact that it captures the complexity levels of aircraft and their behavior during an encounter scenario.

Particularly, for the UEM, Bayesian networks are used to define the Markov’s models for the initial and transition states. Figure 12 demonstrates the Bayesian network for the initial states, whilst Figure 13 illustrates for the transition states. In both networks, the states represented are airspace class (A), altitude layer (L), airspeed (v), acceleration (\dot{v}), turn rate ($\dot{\psi}$), and vertical rate (\dot{h}).

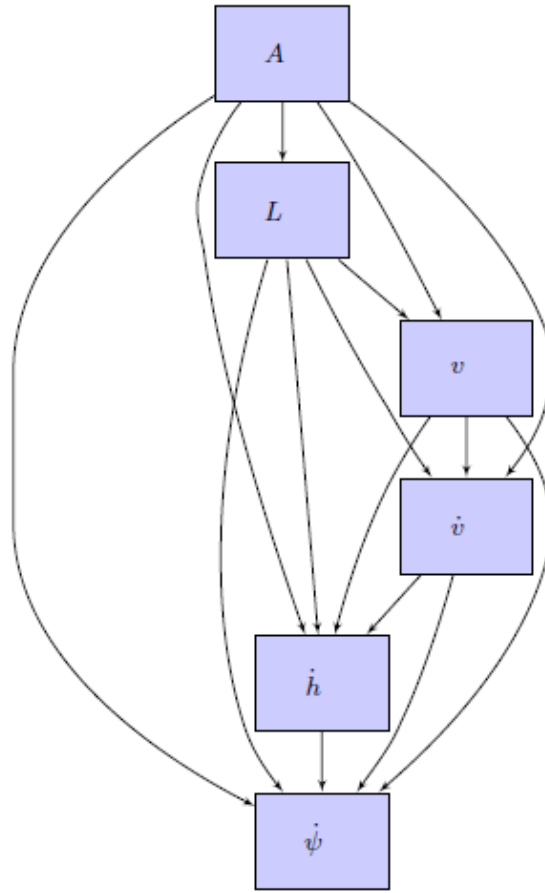


Figure 12: Initial State Bayesian Network for the UEM [27]

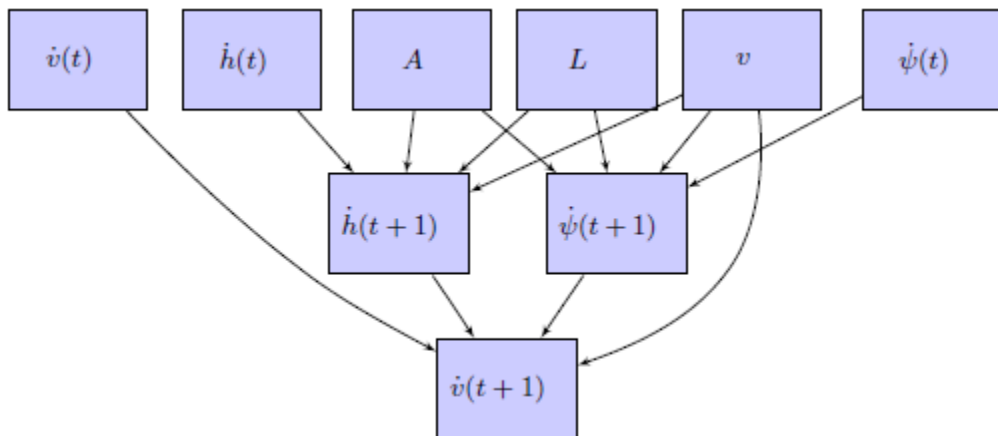


Figure 13: Transition State Bayesian Network for the UEM [27]

The data collected from radars over the NAS is organized into databases of initial and transition states for the Intruder. In order to generate tracks for the simulation for the Intruder, the UEM reads the data from the initial state, Figure 12, for the initial altitude class and layer, airspeed, acceleration and turn rate of the Intruder. Subsequent states are obtained by updating their values with new parameters read from the transition states, Figure 13.

On the other hand, the initial position of the Intruder is uniformly distributed over the Encounter Cylinder, posteriorly rejecting tracks of Intruders not approaching the UAS.

The UAS is initially flying “blind” outside of the encounter cylinder, since the Intruder is outside the radar range of the UAS, whilst the MA is under VFR, seeing each other but without ATC guidance. Further into the simulation, the UAS detects the Intruder when it is within the range of the radar and will maneuver if necessary. The Intruder is assumed to remain “blind” and will not see UAS nor initiate avoidance maneuver.

To calculate the probability of NMAC, the traffic density and pattern of the airspace are required [29].

Several methods are used to predict approaches to collision. Some methods considered for the development of this application are:

- The Big Sky Theory, applied by [17], in which considers the area density constant for a specific area. It also assumes Intruders as stationary in order to simulate collisions with the UAS flying through the airspace, and straight-line flight path, in which assumes the Intruder always has turn rate equals to zero, that is, does not perform any turn during its flight.

- Probabilistic approaches [31], such as Probabilistic Reachable Sets (PRS), in which the statistical probability of the Intruder flight is used to determine the risk. PRS is presented in further details on Section 4.1
- Worst-case scenarios, in which is assumed that the Intruder is always flying in direct collision route to the UAS, as assumed in this thesis in order to calculate the CAT.

The entire flight path for the UAS and Intruder, within the encounter volume defined, were simulated in order to predict the NMAC rate and collision risk. The simulation also evaluates the relative distance and bearing angle between aircraft at every simulation point, as well as predicting flight path for the Intruder. This analysis facilitates the implementation of collision avoidance algorithms.

Point mass flight dynamic models (FDM) are used to simulate the flight path for both UAS and Intruder as described in [31] and [32]. For this project, it is assumed the turn-rate and accelerations are implemented closed-loop, hence eliminating the necessity of FDM for the UAS.

As part of the fault tree analysis, several probabilities of correct operation and failure were considered. As an example, [32] considers probability of detection and false alarm.

To calculate the probability of NMAC the traffic density of the area being analyzed [29] is considered, i.e. the number of aircrafts flying in a determined airspace (aircraft/nm³). Data reported by regulatory agencies will be adopted in order to estimate the traffic density.

The traffic density and initial position of potential Intruder are considered to be uniformly distributed over the Encounter Cylinder. This default assumption is used when representing areas with VFR and precise flights pattern data might not be available.

4.1 Traffic Implementation and Simulation

The system simulation developed in MATLAB includes 60 seconds of data acquired from MIT LL UEM. The system generates initial position and heading angle, as well as its variation for every second, totaling a value superior to the required $2\tau + 15$ seconds proposed by [24].

The required distance for collision avoidance was calculated taking into consideration different velocities for both UAS and Intruder aircraft in all possible bearing angles from Chapter 3, and assuming the worst-case scenario for its flight, that is direct collision route for the aircraft.

With the goal of incorporating Intruders, and using values for distances of $2\tau + 15$ times the relative velocity, the simulations using the UEM were conducted within an Encounter Cylinder of radius 3 nm and height of 200 ft.

The angle of the Intruder when approaching is equivalent at a distance equivalent to $(2\tau + 15) \times v$. Therefore, the distance calculated for $(2\tau + 15) \times v$ is considered to be located within the same bearing angle as the distance measured at $\tau \times v$. Figure 14 demonstrates the approach dynamics between aircrafts in collision route. It is followed by its mathematical determination.

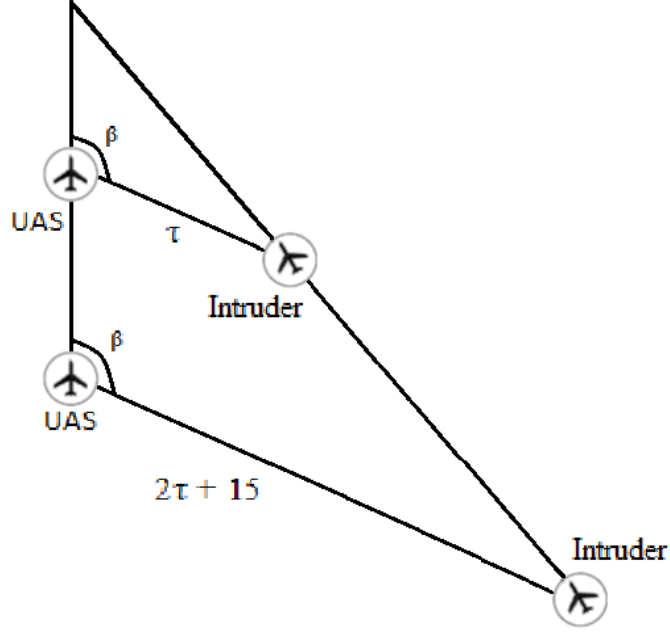


Figure 14: Intruder in collision trajectory bearing angle

The bearing angle is identical for an Intruder in collision route to the UAS. Considering the definition of the Intruder bearing angle at distance $\tau \times v$ as β , and the bearing distance at $(2\tau + 15) \times v$ as β_0 :

$$\beta = \beta_0 \rightarrow \tan^{-1} \left[\frac{y_I - y_U}{x_I - x_U} \right] = \tan^{-1} \left[\frac{y_{I_0} - y_{U_0}}{x_{I_0} - x_{U_0}} \right] \quad (13)$$

Where x_I and y_I are the Intruder longitudes and latitudes at $\tau \times v$; x_{I_0} and y_{I_0} the Intruder longitudes and latitudes for distance $(2\tau + 15) \times v$. Similarly, the variables x_U , y_U , x_{U_0} and y_{U_0} are the equivalent terms for the UAs. Those variables are defined as:

$$x_I = \tau \cdot v_I \cdot \cos\theta_I \quad (14)$$

$$y_I = \tau \cdot v_U - \tau \cdot v_I \cdot \sin\theta_I \quad (15)$$

$$x_{I_0} = (2\tau + 15) \cdot v_I \cdot \cos\theta_I \quad (16)$$

$$y_{I_0} = y_I - (\tau + 15) \cdot v_I \cdot \sin\theta_I \quad (17)$$

$$x_U = x_{U_0} = y_U = 0 \quad (18)$$

$$y_{U_0} = -(\tau + 15) \cdot v_{UAS} \quad (19)$$

Combining Equations (15) and (17), it can be simplified to:

$$y_{I_0} = \tau \cdot v_U - (2\tau + 15) \cdot v_I \cdot \sin\theta_I \quad (20)$$

Substituting the variables above on Equation (13) results in:

$$\beta = \frac{(\tau \cdot v_U - \tau \cdot v_I \cdot \sin\theta_I)}{\tau \cdot v_I \cdot \cos\theta_I} \quad (21)$$

$$\beta_0 = \frac{\tau \cdot v_U - (2\tau + 15) \cdot v_I \cdot \sin\theta_I + (\tau + 15) \cdot v_U}{(2\tau + 15) \cdot v_I \cdot \cos\theta_I} \quad (22)$$

$$\beta = \beta_0 \rightarrow v_U - v_I \cdot \sin\theta_I = v_U - v_I \cdot \sin\theta_I \quad (23)$$

Proving, therefore, that the bearing angle remains unaltered while the Intruder approaches the ownship in a direct collision route.

In addition to the flight simulation, a tracking model was developed in MATLAB. It consists of acquiring 60 data points of a flight pattern from the UEM (1 data point per second).

The dynamic system for tracking is defined using the relative position of the Intruder in the ownship aircraft (UAS) frame. Therefore, in order to derive the Equations for position,

velocity, and relative heading angle, it is necessary to consider the rotation of both aircraft, resulting in the following Equations for longitude, latitude and heading angle, respectively:

$$\begin{bmatrix} \dot{p}_x \\ \dot{p}_y \\ \dot{\theta} \end{bmatrix} = \begin{bmatrix} v_{\text{Intruder}} \cdot \cos\theta - v_{\text{UAS}} + \omega_{\text{UAS}} \cdot p_y \\ v_{\text{Intruder}} \cdot \sin\theta - \omega_{\text{UAS}} \cdot p_x \\ \omega_{\text{Intruder}} - \omega_{\text{UAS}} \end{bmatrix} \quad (24)$$

In the system, p_x and p_y represent the Intruder relative positions in coordinates x (longitude) and y (latitude), respectively, and θ represents the relative heading angle for the Intruder. The velocities (v) and angular velocities (ω) are also considered to simulate and predict flight positions.

Also, in order to measure distance between aircraft and bearing angle, the system measurements are defined as:

$$y = \begin{bmatrix} r \\ \beta \end{bmatrix} = \begin{bmatrix} \sqrt{p_x^2 + p_y^2} \\ \tan^{-1}\left(\frac{p_y}{p_x}\right) \end{bmatrix} \quad (25)$$

Where r represents the distance (range) between aircraft and β is the bearing angle between UAS and Intruder.

Figure 15 shows the comparison of states performed at every iteration between aircraft, checking for relative distance and potential NMAC, and evaluating if the collision risk value is acceptable.

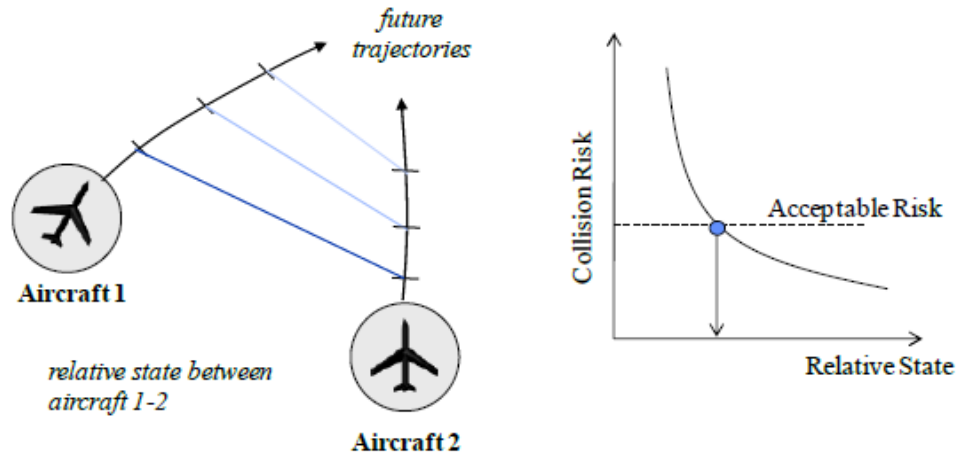


Figure 15: State and risk for the simulation [33]

For every singular event, the bearing angle and velocities are used to calculate the specific value of τ for that scenario. The required time for avoidance maneuver is calculated by the C-based software developed and described on Chapter 3.

In order to evaluate different scenarios of flight, simulations with different ranges of radar were performed. Considering the $2\tau + 15$ seconds' standard for collision avoidance. It is determined the NMAC rate with and without radar detection and avoidance algorithm considering the required distance for avoidance individually determined for each simulation.

As presented on [29], the UEM takes in consideration Altitude class and layer, airspeed, acceleration, turn rate, and vertical rate as variables for the model. With use of initial and transition distribution data, tracks are created following aircrafts tracks observed during actual flights through NAS.

It is noticeable in the model that most Intruders are located as a frontal collision for the UAS, as desired and expected for this analysis. In order to calculate the probability of NMAC it is taken into account the traffic density of the area being analyzed [29].

MIT LL UEM is vastly applied in different analyses. For instance, [33] approaches with the use of 10 million pairs of Monte Carlo simulation, resulting in the estimation of the NMAC risk over different distance and bearing angles between ownship and Intruder, as represented in Figure 16.

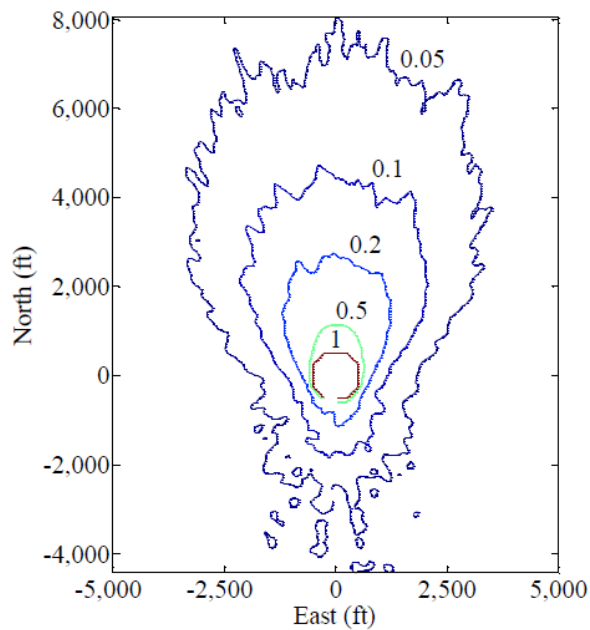


Figure 16: NMAC contours for different distances and bearing angles [33]

It is noticeable that NMAC probability decreases as the distance between ownship and Intruder increases. Also, head-on approaches show a higher density of Intruder flights. Figure 17 demonstrates the risk of NMAC when analyzed as current approach of time. The rate grows

exponentially as distance/time for collision decreases, confirming safety levels proposed by [34] and partially determined by [26].

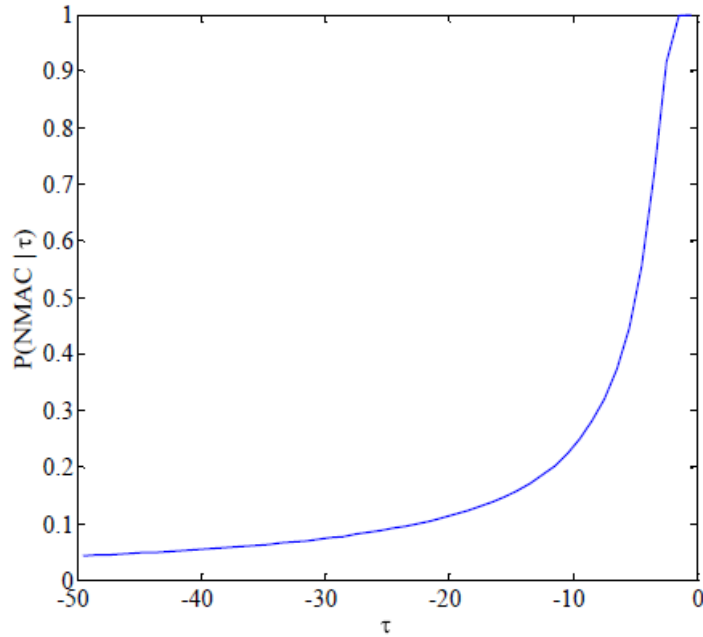


Figure 17: NMAC probabilities for different times to approach (τ) [33]

Several methods are used in order to predict approaches to collision, ranging from considering only the area density, straight line flight path, flight plane sharing to probabilistic or worst-case scenarios methods.

When considering the flight dynamics, reachable sets are defined for different sets of simulation parameters and can be determined as in [32].

Definitions of point flight dynamics are used to simulate flight path for both UAS and Intruder, following procedure described in [31] and [32]. Most analyzes take into consideration point dynamics, neglecting aerodynamics and effects on its flight. Similarly, to the UEM, this thesis adopts kinematic Equations to simulated aircraft trajectories, since the dynamics and

behaviors were already captured from the collection of data points from radars. It also assumed the exclusive use of auto-pilot, resulting in the use of a closed loop system.

[31] defines two different methods of assessing the collision risk: The first is the Maximum Reachable Sets (MRS), which relies on the determination of points where the UAS can reach within a fixed turn rate and velocity over a short period of time. An example of obtained MRS is shown in Figure 18.

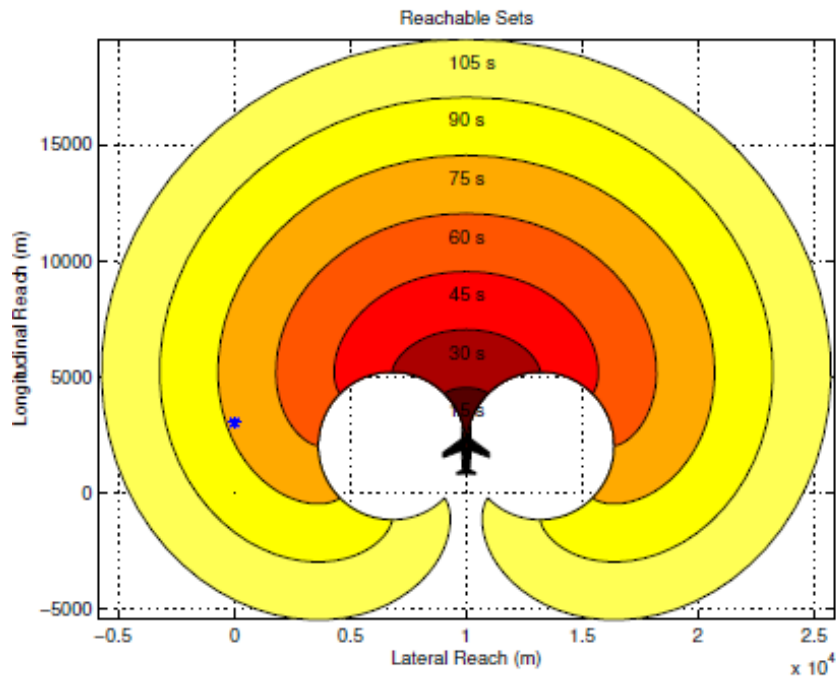


Figure 18: MRS for different values of turn rate [31]

The second method is the PRS. It relies on typical flight dynamics observation to set boundaries according to observed probabilities of trajectories. Figure 19 demonstrates an example of this method obtained on [31].

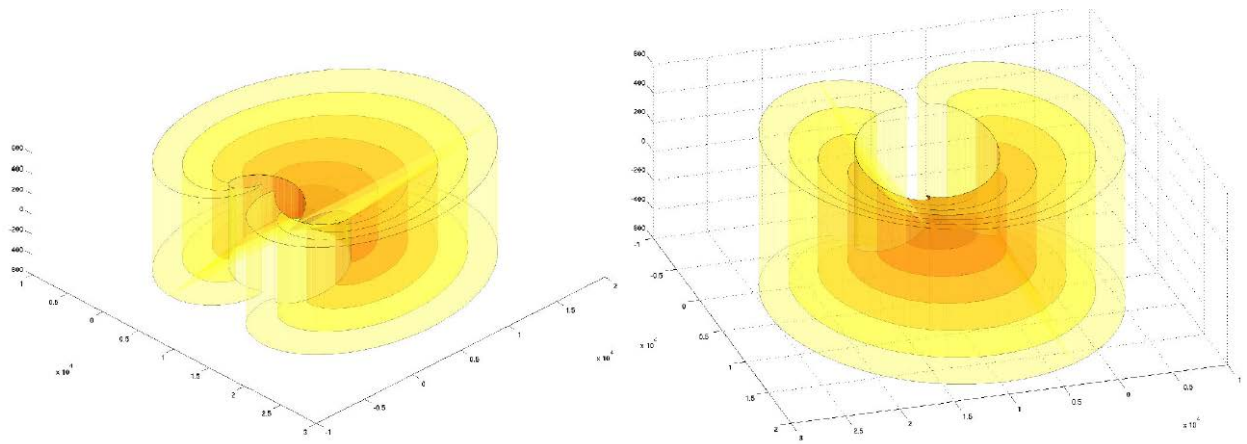


Figure 19: PRS examples in a three-dimensional case [31]

The PRS approach determines three-dimensional boundaries considering probabilities for different bearing angles and altitude differences. The general result can be used to predict, compare and validate results from a future precursor development of the CAT with collision avoidance method used in this thesis for the three-dimensional analysis.

With use of the encounter model developed based on MIT LL model, it is possible to determine the NMAC rate, as well as required distances for radar detection when operating UAS at BVLOS applications in the Canadian Airspace.

Chapter 5

Collision Risk Analysis

Chapter 5 will present a detailed analysis and results for the implementation of the model developed in this thesis. Different scenarios are simulated considering locations, altitudes and conditions for the airspace in which the UAS is operating.

UAS should fulfill the requirement to not increase the NMAC rate in the airspace in which it is inserted. Also, risk analysis for UAS should consider potential damage to other aircraft and hazards posed to population and constructions on the ground.

It is important to notice that, despite accounting for mitigation effects, the model for risk estimation make assumptions to simplify its determination, consequently imposing limits for its possible applications. For instance, the model described in [15] does not consider demographic density variation, whilst [17] determines density by published census data.

In a complete UAS system, in which considering an implemented DAA system, the fault tree is defined analogously to [17] by the Equation:

$$P_{\text{NMAC}} = P_{\text{SEP LOSS}} \cdot P_{\text{UAS FAIL}} \cdot P_{\text{MA FAIL}} \quad (26)$$

Where P_{NMAC} represents the probability of NMAC posteriorly calculated, $P_{\text{SEP LOSS}}$ is the probability of separation loss occurring, $P_{\text{UAS FAIL}}$ is the probability of the UAS system failing to detect or avoid the Intruder, and $P_{\text{MA FAIL}}$ is the probability that the Intruder MA do not detect or avoid the UAS. If there is no implementation of DAA applications for the Intruder, $P_{\text{MA FAIL}}$ is considered to have a unit value.

From the Fault Tree for this system, the DAA failure component is equivalent to $P_{UAS\ FAIL}$, the probability that the Intruder will be entering the Encounter Cylinder is $P_{SEP\ LOSS}$, whilst the NMAC rate is P_{NMAC} .

It is important to observe that the probabilities of failure described above are not independent. That is, components that might lead to a collision in the Fault Tree possess dependency, resulting in a system which is too complex to be determined without simulation. From Equation (26), the probabilities $P_{UAS\ FAIL}$ and $P_{SEP\ LOSS}$ can't be calculated independently.

Therefore, it is necessary to implement the simulation (MIT/LL UEM) with data from radars in the real airspace in which the system will be implemented.

When accounting for risk, as pointed out in [18], the bearing angle of the Intruder is an essential aspect to be observed. This allows efforts to be focused on detection and avoidance of collisions in specific bearing angle sections.

As an initial analysis, Intruders were divided into different altitude levels: From 3,000 ft.-5,000 ft., and above 5,000 ft. In both scenarios, the Intruder is simulated with its origin in the Encounter Cylinder previously defined.

As expected, there is a higher concentration of NMAC for Intruders with a frontal bearing angle, due to its higher relative velocity and traffic pattern. In addition, the results present a slightly lower number of NMAC for flights in the higher altitude layer.

In order to estimate the value of encounters per hour in a determined area, it is necessary to take into account the flight density of that particular airspace. As defined in [27], the NMAC rate, λ_{NMAC} , is determined by:

$$\lambda_{NMAC} = P(NMAC|ENC) \cdot \lambda_{ENC} \quad (27)$$

Where $P(NMAC|ENC)$ is the percentage of NMAC given that the Intruder is within the Encounter Cylinder previously calculated, and λ_{ENC} is the rate of Intruders penetrating the volume swept by the UAS multiplied by the constant air traffic density of the specific area under analysis, being posteriorly analyzed in further detail.

Using flight statistics collected for periods in December 2007 and June 2008 by FAA and adopted by MIT/LL in [27], when analyzing the risk in the NAS, the traffic density is determined in. Figure 20 illustrates the distribution of density through the NAS for flights between 3,000 ft. and 5,000 ft.

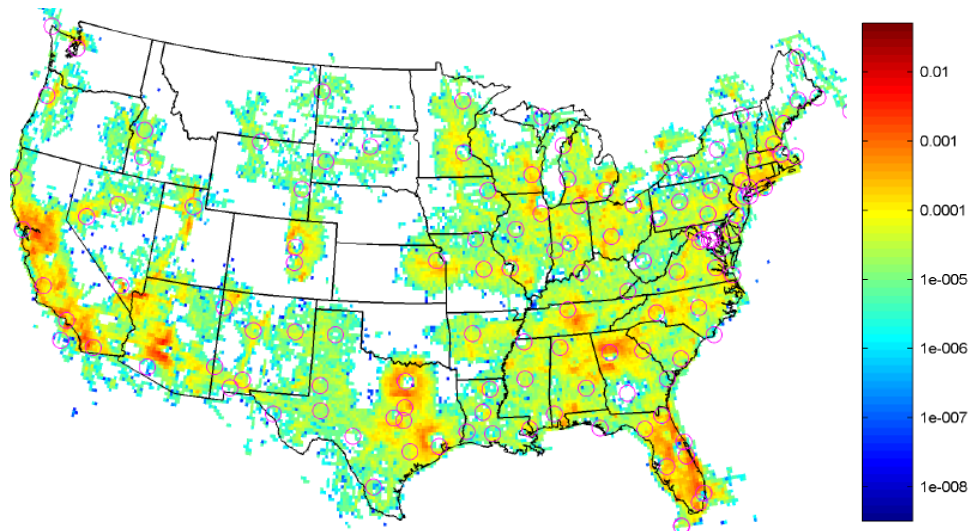


Figure 20: Aircraft density over the NAS in aircrafts/nm [27]

It is also observed that different altitude levels affect the NMAC risk. That is, higher flight levels present a lower density for most regions in the NAS, and, therefore, are an important factor

to be considered when defining the operation of a UAS in a certain region. Figure 21 presents the air traffic density when considering altitudes between 10,000 ft. and FL180 (Flight Level 18,000 ft.).

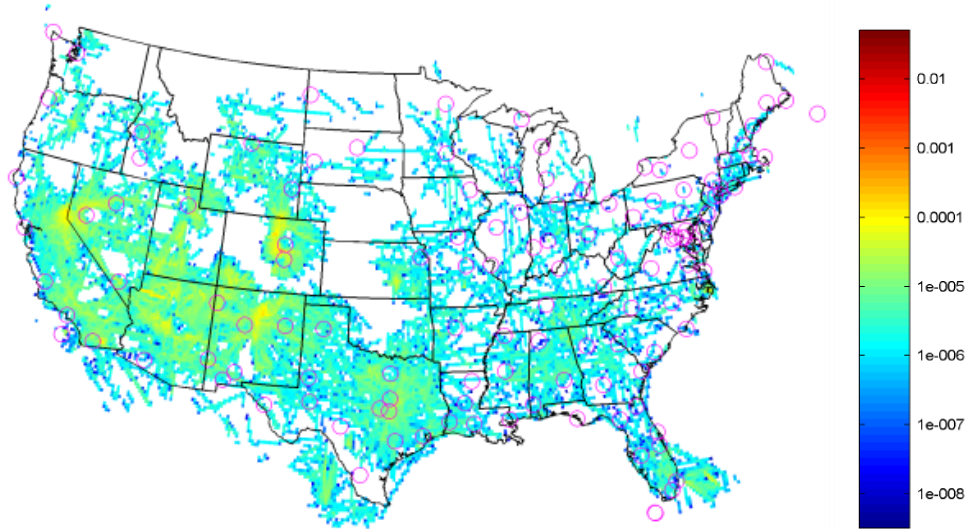


Figure 21: Aircraft density over the NAS in aircrafts/nm between 10,000 ft. and FL180 [27]

After performing 1 million encounter simulations for each altitude layer, 708 head-on collisions (bearing angles between -60° and 60°) occurred for flights between 3,000 ft. and 5,000 ft., whilst 695 NMAC were simulated for flights above 5,000 ft.

The amount of collisions progressively alters with change in the bearing angle. When considering flights above 5,000 ft., 365 NMAC occurred with the Intruder between 60° and 120° (side-on), and 137 NMAC for Intruders at tail-chase (bearing angle between 120° and 240°).

Figure 22 demonstrates the distribution of NMAC above 5,000 ft. with the UAS flying without any detection or collision avoidance implementation.

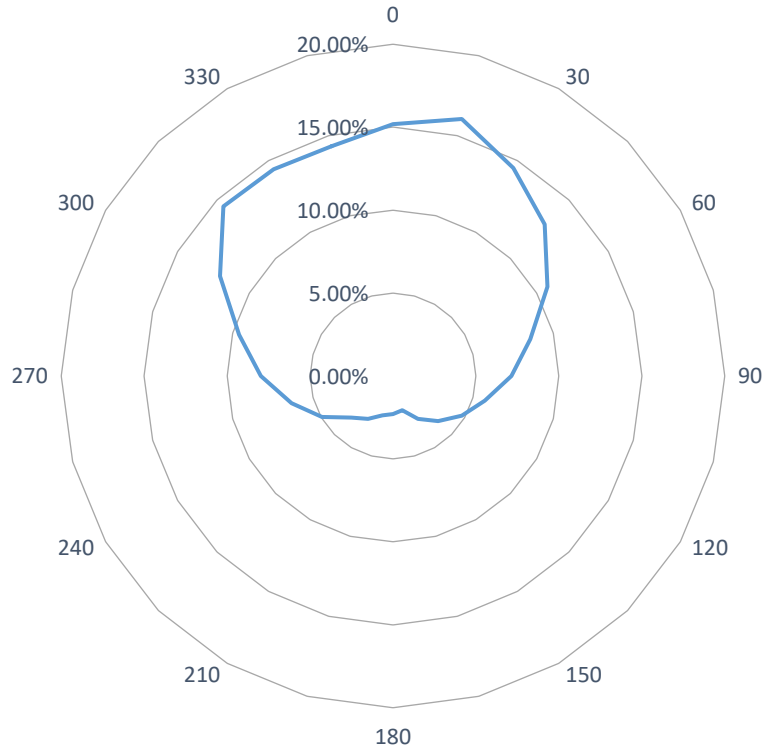


Figure 22: Intruder bearing angle distribution

Considering all bearing angles for flights inside the Encounter Cylinder, 0.235% of the total number of flights simulated in the lower altitude layer and 0.229% of flights simulated in the higher altitude layer are NMAC trajectories. From the collision trajectories, a total of 57.78% are concentrated on head-on collision bearing angles, while only 11.98% are originated from the tail-chase scenario.

As an example analysis, the encounter rate for UAS flying over Michigan's Upper Peninsula, specifically in the Marquette County Area, is determined to be $2.144 \cdot 10^{-5}$ NMAC/hour, whilst flights around the Miami Metropolitan Region present a risk in the order of $6.432 \cdot 10^{-4}$ NMAC/hour for flights between 3,000 ft. and 5,000 ft.

The encounter rates determined above are not within desired accepted safety levels previously determined (10^{-7}). Therefore, for applications in areas with a higher air traffic density (more populated areas), it is necessary to implement capabilities to decrease the rate, that is, DAA systems.

Since there is a small variation between Intruders from altitude layers of 3,000 ft.-5,000 ft., and above 5,000ft., subsequent simulations will be performed adopting altitudes superior to 5,000 ft., where most of the UAS operate due to the lower air traffic density and, consequently, the lower risk introduced to the airspace.

In Equation (27), the rate of Intruders penetrating the Encounter Cylinder is determined by the aircraft density (ρ) for a specific airspace in aircrafts/nm³, multiplied by the Encounter Cylinder swept volume (V):

$$\lambda_{ENC} = \rho \cdot V \quad (28)$$

The Canadian rate of collisions is defined in [35]. For MA, the Canadian Airspace registered $5.1 \cdot 10^{-5}$ accidents/hour in 2014. TSB also states:

- 14% of collisions are en route, and are therefore covered in this analysis.
- 1% of accidents are collisions of aircraft.

Further, TSB specifies that 14% of accidents are due to a Loss of Separation, and these are not considered in this analysis, because it is unclear what standardized separation distance was used to constitute as a loss of separation in the report. Therefore, only collisions are counted.

Finally, applying the estimation from FAA and adopted by [24], where 1 in 10 aircraft that penetrate the NMAC volume results in a collision, the NMAC rate is estimated as:

$$\lambda_{NMAC} = 5.1 \cdot 10^{-5} \cdot 14\% \cdot 1\% \cdot 10 \quad (29)$$

$$\lambda_{NMAC} = 7.14 \cdot 10^{-7} \text{NMAC/h} \quad (30)$$

It is important to observe that this rate includes both GA and airliner traffic, operating under Instrument Flight Rules (IFR) and VFR for all classes of airspace. It also does not include unreported accidents. Consequently, the NMAC rate has a built-in conservatism, since GA has historically presented a higher NMAC rate than aircraft flying with IFR or VFR.

Following the $2\tau + 15$ seconds standard for the minimum collision avoidance distance, simulations were performed with use of different ranges of radar detection. Using fast-simulation of over 1 million flights for a chosen airspace density and for a given radar detection range. A NMAC has occurred in the case that the radar range is smaller than the required minimum collision avoidance distance determined by the $2\tau + 15$ seconds standard.

In case the detection range calculated is smaller than the required avoidance maneuver time determined by the $2\tau + 15$ seconds standard is executed. The avoidance heading angle is defined by verifying possible avoidance routes and selecting a heading angle in which there is a lower risk of collision. Figure 23 demonstrates a scenario in which the radar detection is appropriate for the intruder distance, and the UAS avoidance maneuver is successfully performed. It is included the UAS performing the avoidance (turn heading to 90°), the predicted trajectory for the Intruder, and the actual location of the Intruder.

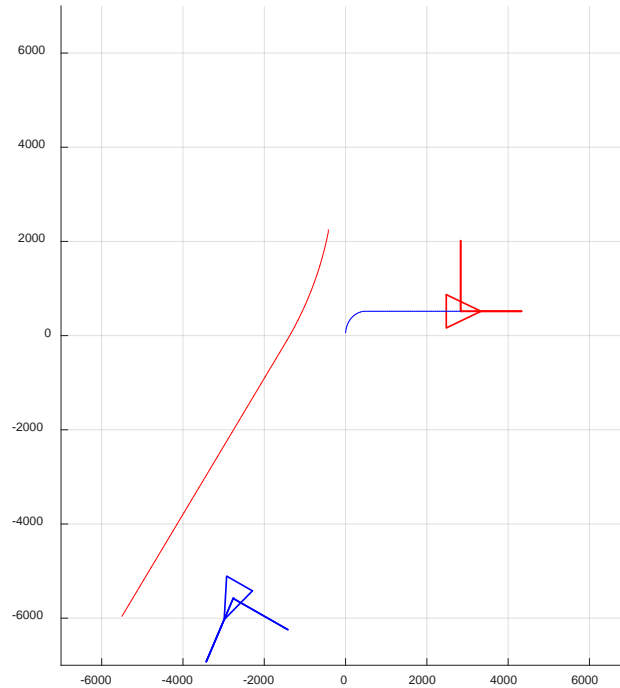


Figure 23: Avoidance maneuvering performed by the UAS

Initially, a radar capable of detecting Intruders in frontal and lateral headings, that is at angles between $\pm 120^\circ$, was considered since tail-chase collisions constitute a lower probability and require a smaller distance for avoidance.

The graphs on Figures 24, 25, 26, and 27 demonstrating the reduction in collision by the use of collision avoidance maneuvering are generated by recording the amount of NMAC for each 30° section of bearing angles, including all simulated detection ranges for the radar.

Figure 24 demonstrates the distribution of NMAC in different bearing angles and different radar ranges, obtained statistically over 1 million encounters for each detection range. The UAS was initially flying north (0°) at a velocity of 100 kt., with a maximum turn rate of 2G ($6^\circ/s$) and at an altitude above 5,000 ft. Also, the Intruders are limited to under 170 kt.. The probability

distribution in Figure 24 is for radar ranges of: (a) no radar, (b) 0.25 nm, (c) 0.5 nm, (d) 1 nm, (e) 1.5 nm, (f) 2 nm, (g) 2.5 nm and, (h) 3 nm.

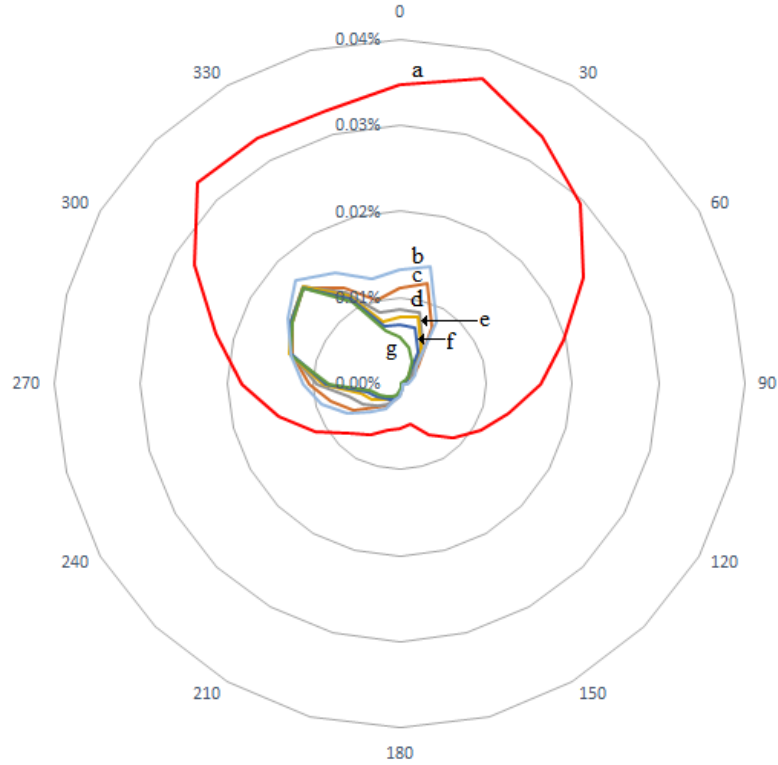


Figure 28: NMAC distribution for different radar ranges with ± 120 detection.

The incorporation of radar into collision avoidance maneuvering resulted in a reduction of NMAC rates for head-on bearing angles. Critical bearing angles previously addressed (between 60° and 90° , and its pair from 270° to 300°) represent a higher probability of collisions, since these indicate that requires a greater distance in order to successfully perform avoidance maneuvers.

Figure 25 shows the NMAC percentage decrease for different ranges of detection. Incorporating radar with a detection range of 0.25 nm for the frontal $\pm 120^\circ$ results in a collision reduction of 69.23% compared to flights without any detection capability. Increasing the radar

detection range to 3 nm with the same angular detection scope results in a total reduction of 80.77%.

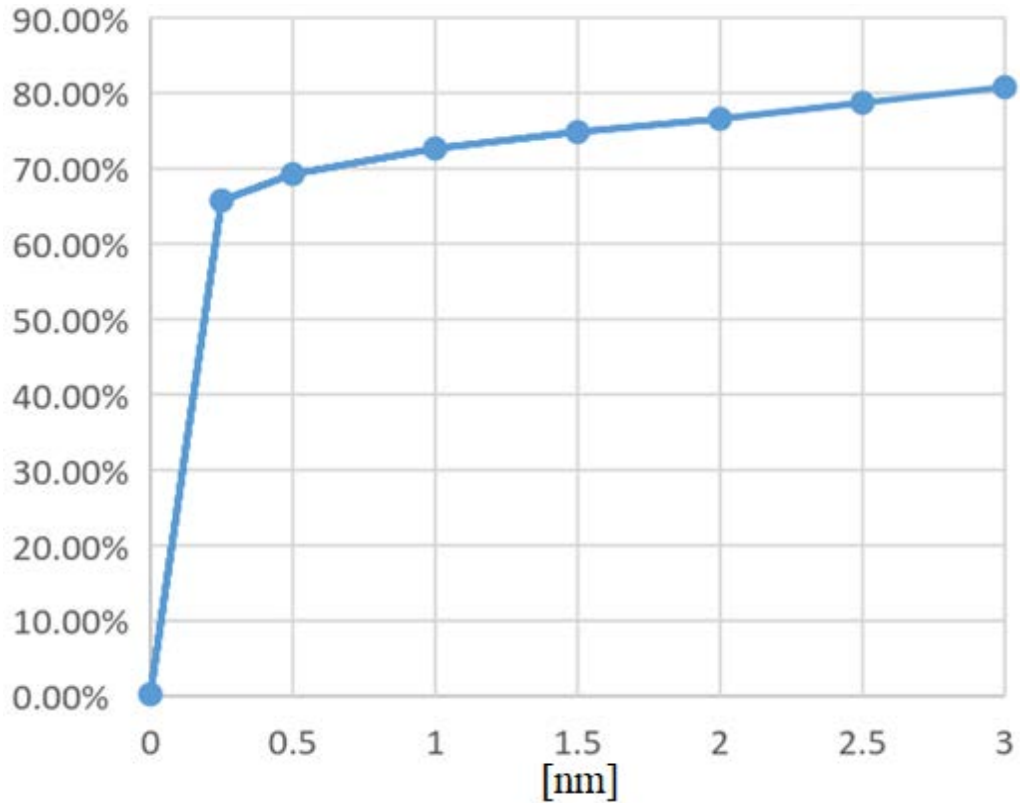


Figure 29: NMAC reduction for different radar ranges with ± 120 detection

The same procedure was replicated for the simulation using radars ranging from 0.25 nm to 3 nm but with the ability to detect Intruders from all bearing angles. Figure 26 demonstrates the NMAC rates, considering 1 million encounters simulated for each radar detection range.

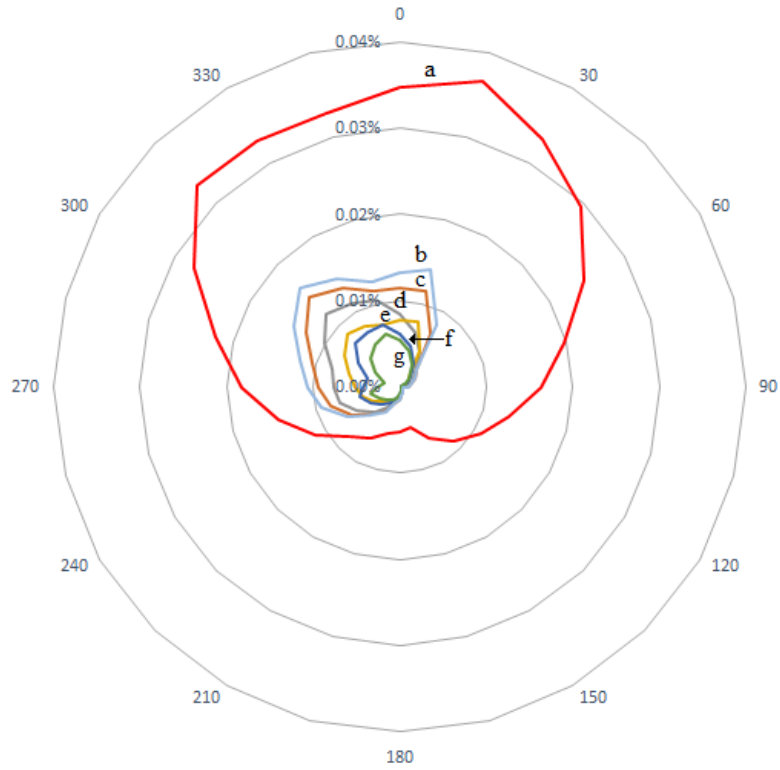


Figure 30: NMAC distribution for Intruders with 360° detection.

From Figure 26, the use of 360° radars results in a lower amount of NMAC rate than in previous applications with $\pm 120^\circ$ detection angles. The NMAC percentage was reduced by 69.97% for a radar detection range of 0.5 nm compared to flights without any detection capability. Increasing the detection distance to 3nm, results in a total reduction of 92.13%. The reduction in NMAC rates for 360° radars is demonstrated in Figure 27 for different detection ranges.

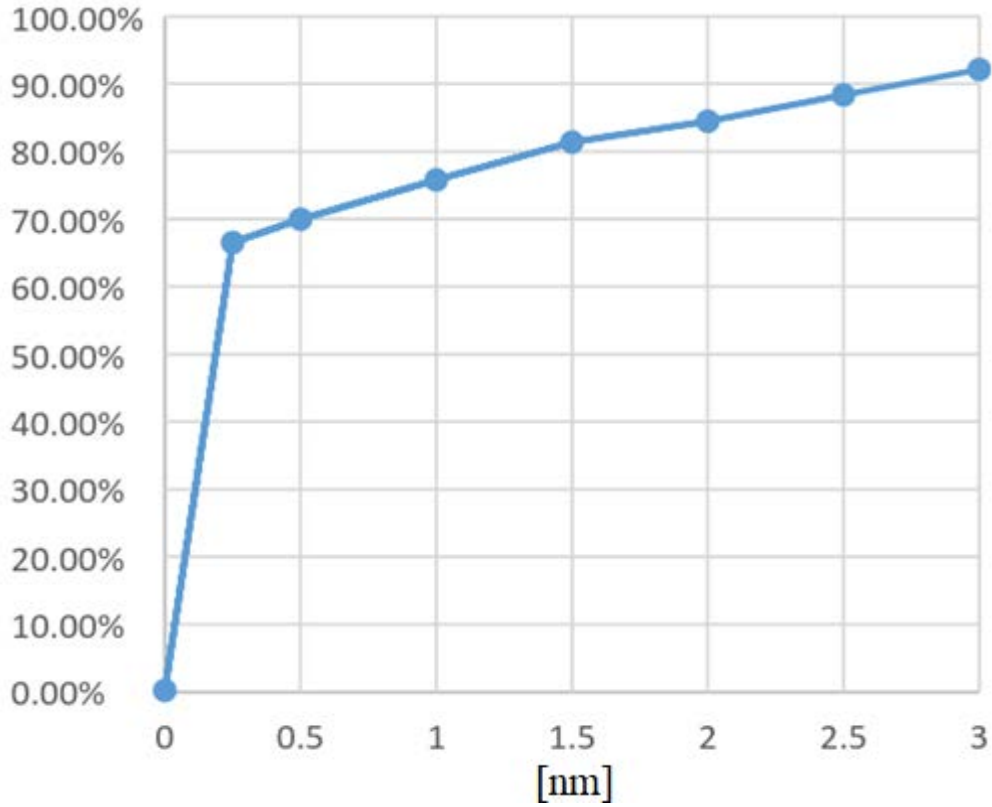


Figure 31: NMAC reduction for different radar ranges with detection of all bearing angles.

Using the previously defined risk calculated for Canada [35], and back calculating, the average aircraft density for the entire Canadian airspace, by Equations (27) and (28), is determined to be:

$$\lambda_{ENC} = \lambda_{NMAC}/P(NMAC|ENC) = 3.17 \cdot 10^{-4} \quad (31)$$

$$\rho = \lambda_{ENC}/V = 8.46 \cdot 10^{-6} \text{aircraft}/nm^3 \quad (32)$$

The overall density for the Canadian Airspace, without considering a specific region, is equivalent to the density observed in American states such as Indiana and Kentucky. Therefore,

simulation will be based on statistics from these regions used in the UEM, since specific Canadian flight data and densities are not available.

The NMAC probability for the average Canadian airspace calculated is reduced from $7.14 \cdot 10^{-7}$ NMAC/hour to $3.04 \cdot 10^{-7}$ NMAC/hour when adopting a radar with a 0.25 nm range, and to $1.07 \cdot 10^{-7}$ NMAC/hour when applying radar with a detection range of 3 nm.

That represents a reduction of 57% for a radar detection range of 0.25 nm compared to flights with no detection capability. Incrementing the detection distance to 3nm, it results in a total reduction of 93%. Both scenarios, the model uses full coverage of the radar. Also, these values are well below the Canadian National level currently observed for MA.

Assuming an efficiency rate of the radar detection other than 1, will result in a slight change in NMAC rate. Adopting a value of $P_{UAV\ FAIL} = 0.95$ for the previously simulated scenario with DAA implementation, the probability for Canada becomes $2.98 \cdot 10^{-7}$ NMAC/hour for a 0.5nm detection range, and $1.38 \cdot 10^{-7}$ NMAC/hour for a 3 nm radar range.

Since most simulated flights have velocities under 170 kt., the Intruder velocity is limited to 170kt. in the simulation. Resulting a higher avoidance rate for DAA capabilities for systems with a greater detection range (above 2.5 nm). Figure 28 illustrates the distribution of aircraft velocities. It is noticeable that a small percentage of aircraft are faster than 170 kt., which are made mostly of commercial aircraft, not included in this particular study.

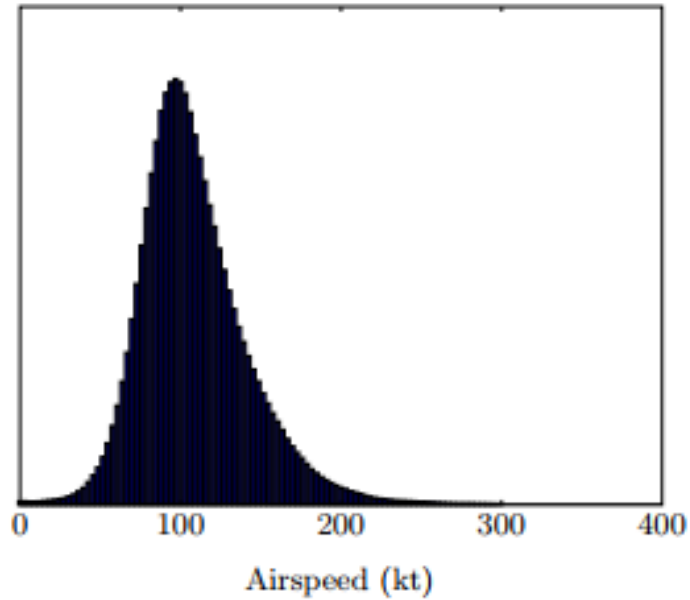


Figure 32: Distribution of velocities observed in NAS uncontrolled airspace [27]

Assuming operations where Intruder aircraft are limited to velocities under or equal to 170 kt., higher altitudes (above 5,000 ft.), and simulating therefore an environment with lower traffic density, the improvements from the collision avoidance algorithm are more accentuated. Figure 29 illustrates the risk of NMAC for Intruder aircraft flying inside the Encounter Cylinder. The model considers UAS possessing radar detection ranges from 0.25 nm to 3 nm, and detection angles in the section of $\pm 120^\circ$. It is observed, the NMAC risk decreasing progressively along with increase in range.

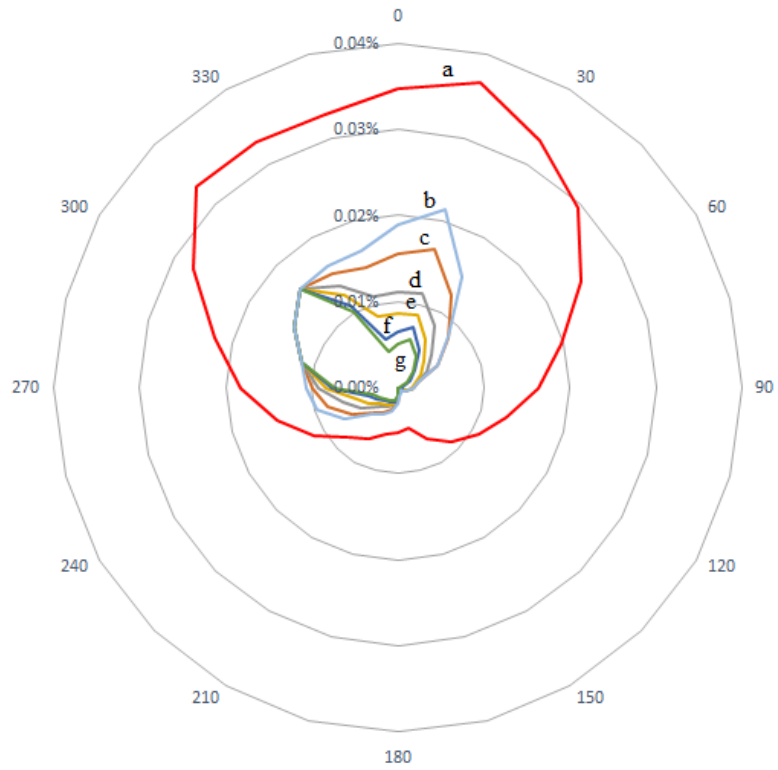


Figure 33: NMAC probability distribution for Intruders limited to 170 kt.

NMAC rates in this scenario can be reduced up to 84.95% when adopting a radar with detection range of 3 nm, whilst 0.5 nm already generates a reduction of 61.83%. The graph in Figure 30 demonstrates the gradual reduction of accidents with an increase in the detection range.

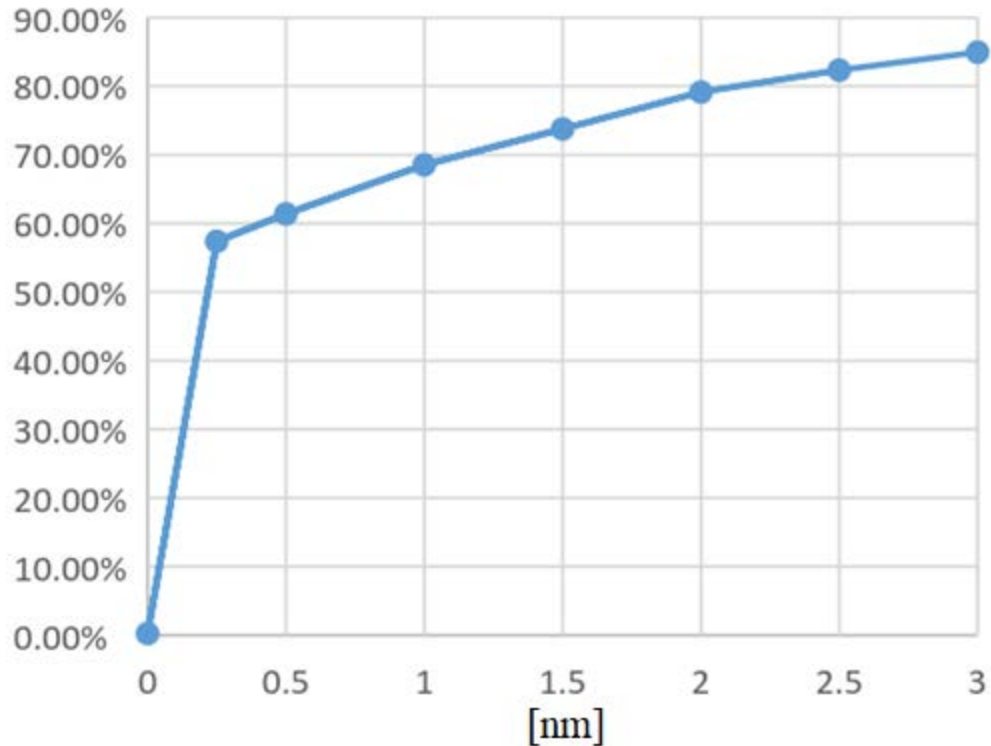


Figure 34: NMAC reduction with $\pm 120^\circ$ detection and velocity limited to 170 kt.

It is noticeable that, in this particular simulation, a significant gain in avoidance occurs between 2.5 nm and 3 nm, differently from previously presented results. This fact occurs since Intruders with higher velocities are the aircraft resulting in a higher NMAC rate since they require a larger amount of time and distance in order to fulfill the avoidance maneuver requirements successfully.

Figure 31 demonstrates the distribution of NMAC for different bearing angles and different radar ranges, performing 1 million encounters for each detection range. The model considers an UAS flying initially north (0°) at a velocity of 100 kt., turn rate of 2G ($6^\circ/s$), and with altitude above 5,000 ft. Also, the Intruders are limited to a velocity of 170 kt.. The model includes the

probability distribution for applications without a radar (outer contour) and radar ranging from 0.25 nm (a) to 3 nm (g).

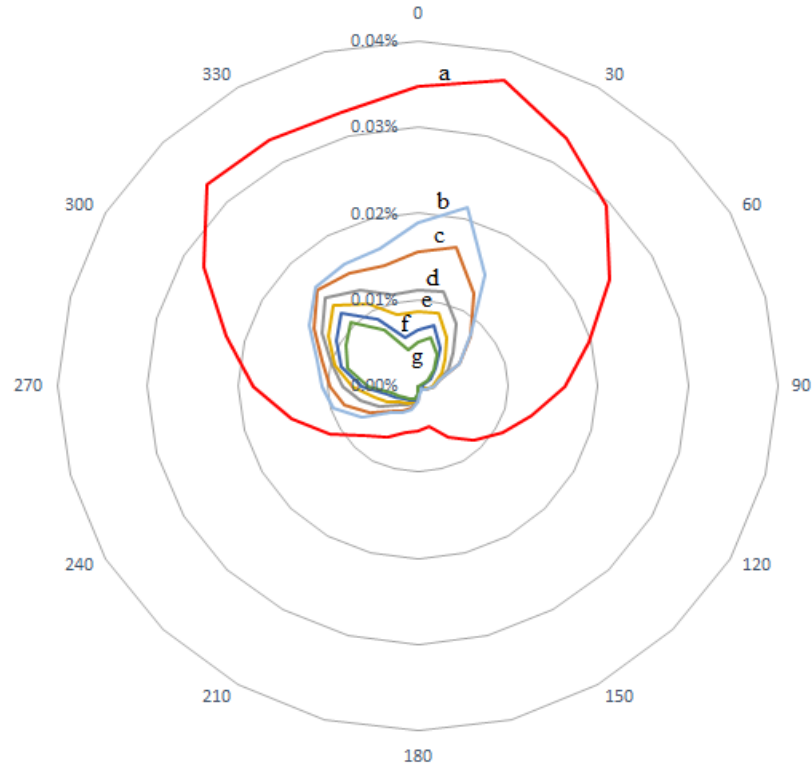


Figure 35: NMAC distribution for Intruders limited to 170 kt. with 360° detection.

The incorporation of radar into collision avoidance maneuvering resulted in a reduction of NMAC for head-on bearing angles. Critical bearing angles previously addressed (between 60° and 90°, and its pair from 270° to 300°) represent the higher probability of collisions, since it requires a greater distance in order to successfully perform the avoidance maneuvering

For this scenario can be reduced up to 93.16% when adopting a radar with detection range of 3 nm, whilst 0.25 nm already generates a reduction of 57.43%. The graph in Figure 32 demonstrates the gradual reduction of accidents with the increase of the detection range. Similarly,

to the previous scenario, a significant NMAC reduction is observed for larger values of detection range.

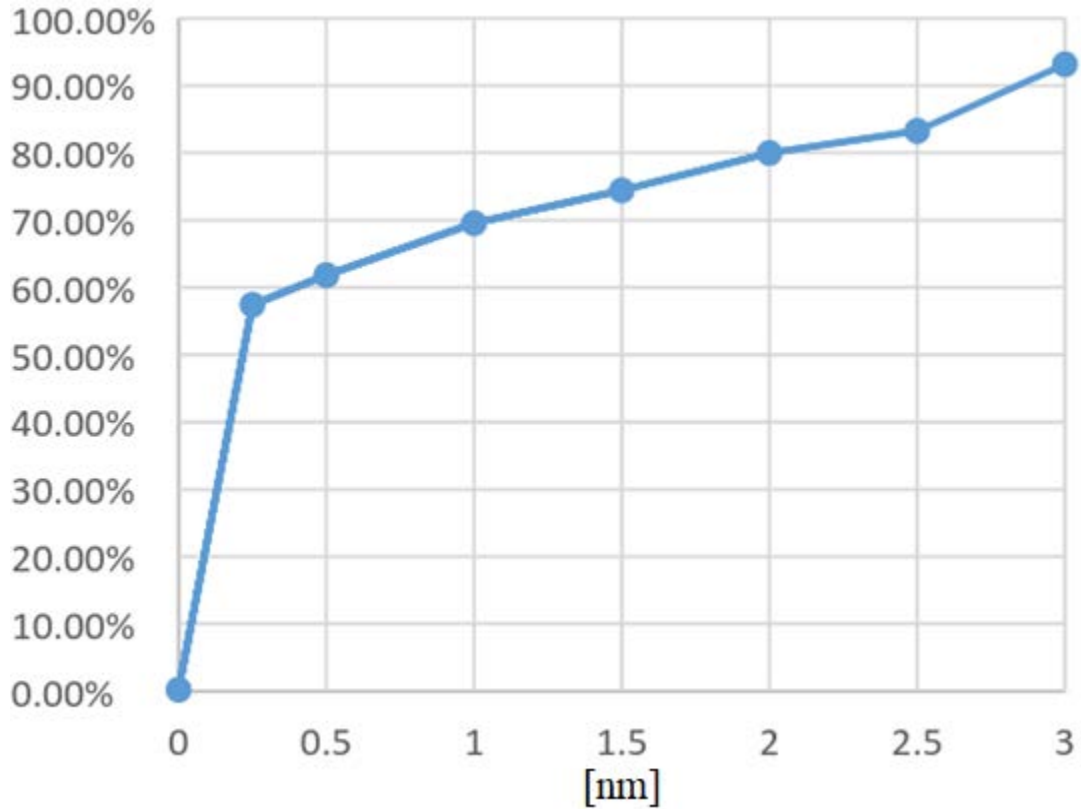


Figure 36: NMAC reduction with 360° detection and velocity limited to 170 kt.

Using the previously defined risk calculated for Canada, and applying Equations (27) and (28), the NMAC probability is calculated to be reduced from $7.14 \cdot 10^{-7}$ NMAC/hour to $3.04 \cdot 10^{-7}$ NMAC/hour when adopting a radar with 0.25 nm range, and to $1.07 \cdot 10^{-7}$ NMAC/hour applying a radar with detection of 3 nm.

That represents a reduction of 57.43% for a radar detection range of 0.25 nm compared to flights without any detection capability. By incrementing the detection distance to 3nm, a reduction

of 93.16% is obtained. Both values are well below the Canadian National level currently observed for MA.

Assuming an efficiency rate of radar detection other than 1 will, result in a slight change in NMAC rate. Adopting a value of $P_{\text{UAV FAIL}} = 0.95$ for the previously simulated scenario with detect and avoid implementation, the probability for Canada becomes $2.98 \cdot 10^{-7}$ NMAC/hour for 0.5nm detection range, and $1.38 \cdot 10^{-7}$ NMAC/hour for a 3 nm radar range. Both values still present significant safety gains when compared to the Canadian National Average air traffic.

The graph in Figure 33 demonstrates the gradual reduction of accidents with the increase of the detection range. Scenarios with radars detecting frontal and lateral bearing angles ($\pm 120^\circ$) and complete circumference (360°) are included. Also, it is considered both scenarios with full range of Intruder velocities, as well as limited to 170 kt..

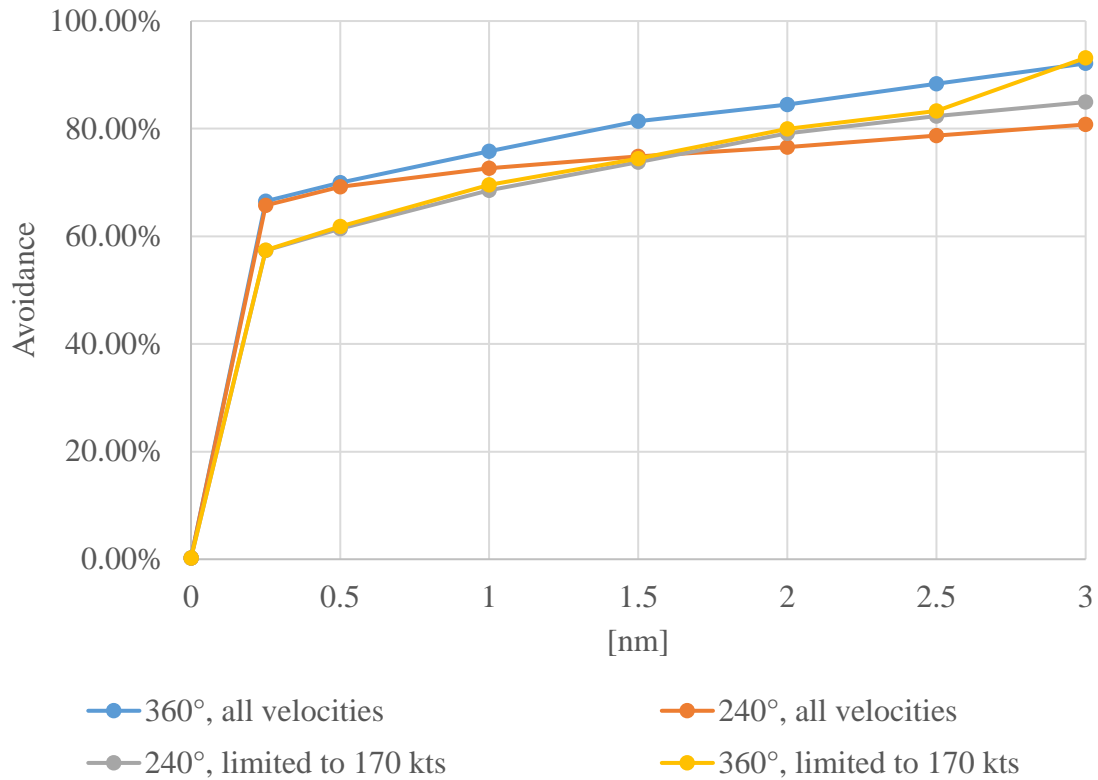


Figure 37: NMAC reduction with 360° detection and velocity limited to 170 kt. under 5,000ft.

A significant avoidance gain occurs between 2.5 nm and 3 nm was noticed when simulating with a complete circumference radar detection and Intruder velocity limited to 170kt., differently from the other presented results. This occurs since Intruders with higher velocities are causing NMAC since it requires a larger amount of time and distance in order to fulfill the avoidance maneuver requirements.

Figure 34 compares the NMAC rates for regions with different air traffic density ($5 \cdot 10^{-5}$, $2.5 \cdot 10^{-5}$ and $5 \cdot 10^{-6}$ aircraft/nm³) to the reported Canadian rate for 2015. The curves demonstrate NMAC reduction for different values of radar detection (from no detection to 3 nm) with an

angular detection of $\pm 120^\circ$ and assuming Intruders with velocity limited to 170 kt., following assumptions adopted by [1].

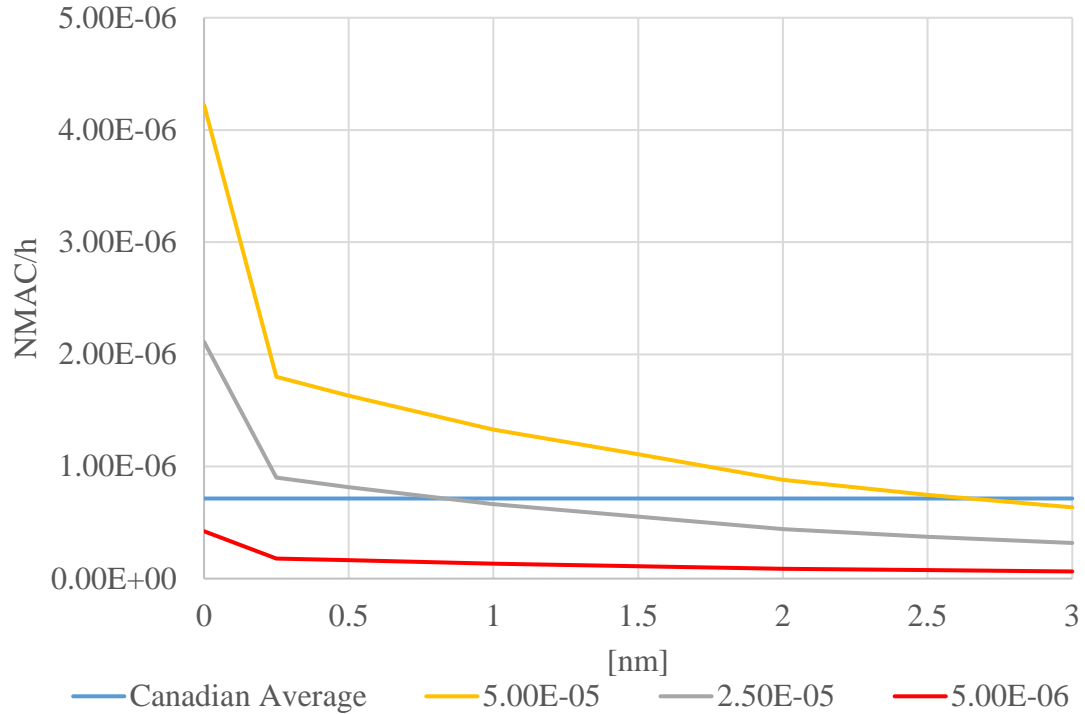


Figure 38: NMAC rates for different densities

Without using radar for DAA, both $2.5 \cdot 10^{-5}$ and $5 \cdot 10^{-5}$ aircraft/nm³ density areas present NMAC rate higher than Canada’s NMAC reported for 2015, while $5 \cdot 10^{-6}$ aircraft/nm³ density areas do not require any DAA to match the Canadian NMAC rate.

With adjusted radar range, UAS can operate at all regions with NMAC rate below the National Average for MA. For instance, regions with density of $5 \cdot 10^{-6}$ and $2.5 \cdot 10^{-5}$ aircraft/nm³ require detection ranges of 2.5 nm and 1 nm, respectively.

It was also estimated the levels of safety when analyzing Canadian provinces individually. Figure 35 compares the NMAC rates in different regions (British Columbia, Ontario, Nova Scotia and Newfoundland). The traffic densities are estimated adopting the procedure proposed by [17], considering Intruders with velocity limited to 170 kt., and evaluating detection ranges from 0.25 nm to 3 nm. It assumes radar angles for $\pm 120^\circ$. The results are compared with the Canadian NMAC rate for 2015.

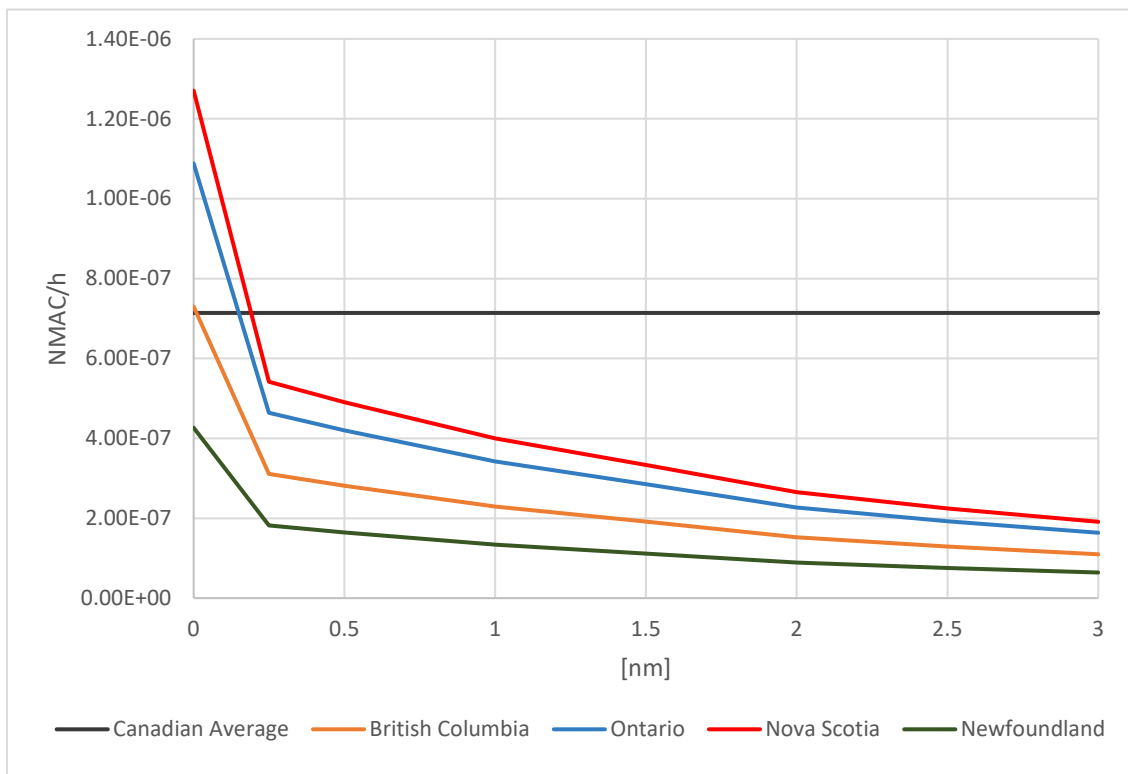


Figure 39: NMAC rates for detection angles, ranges and locations in Canada

Originally, both Ontario and Nova Scotia present NMAC rate higher than Canada's NMAC reported for 2015, whilst British Columbia presents a slightly higher estimated NMAC rate.

With the implementation of radars for the performance of collision avoidance maneuvers, the rates for all provinces achieved levels under the national average for 0.25 nm. For instance, a radar detection of 0.25 nm results in a NMAC rate 24% smaller than the Canada's reported rate for Nova Scotia. The rates for Ontario, British Columbia and Newfoundland are 35%, 56% and 75% smaller than the National average, respectively.

The developed method can also determine gains from the increment of the radar detection to a 3 nm range. In that case, the rates are reduced from the national average by 73% for Nova Scotia, 77% for Ontario, 85% in British Columbia and 91% in the island of Newfoundland.

It is verified, therefore, the viability of UAS applications in the Canadian airspace in general with higher levels of safety, and requiring, in some cases, the addition of radar detection and DAA capability to match and reduce the currently observed NMAC rate.

5.1 Canadian Arctic Surveillance Application

The method developed was applied for analysis of NMAC rates for TC in the Canadian Arctic. The operation consists of a Medium Altitude Long Endurance (MALE) UAS performing surveillance between the airports of Iqaluit (in Nunavut) and Inuvik (in the Northwest Territories), with flights at altitudes between 2,000 ft. and FL200. The trajectory, therefore, consists of 200 nm located in latitudes between 60° and 70° north.

Analyzing flight reports over a year long period in selected arctic regions, the NMAC rate for the operation is calculated, as well as recommendations for flight levels with lower aircraft densities.

As a preliminary analysis, it can be determined that, for an UAS flying at 100 kt., with a turn rate limited to 2G ($6^\circ/s$), Intruder aircraft velocities smaller or equal to 170 kt., and assuming that most of Intruder aircraft are at altitudes equal or lower than 18,000 ft., the NMAC rate is estimated as $3.52 \cdot 10^{-7}$ NMAC/h.

Therefore, the predicted NMAC rate is 50.7% below the Canadian National Average for 2015, which includes GA, and commercial flights, and is, therefore, a conservative estimation for the uncontrolled airspace scenario.

The preliminary analysis conducted by the implementation of the developed model concludes that the Arctic surveillance operation presents a low risk and can be conducted without the requirement of implementing DAA capabilities, consequently reducing the development and implementation costs associated with the project.

Further investigations and analyses are being conducted, evaluating risk and NMAC rate for specific operations with a higher detail resolution.

Chapter 6

Conclusion

MOPS and ranges estimations for radars in UAS flying BVLOS in GA were determined following the NRC recommendations [24]. Simulations were used to estimate NMAC rates for UAS with and without DAA capabilities.

This thesis developed a new methodology and application from the widely accepted and implemented MIT/LL encounter model to estimate a Canadian NMAC rate using on an avoidance standard proposed by NRC. Based on previous developments and analysis performed in academia and aviation agencies from several countries, a new methodology was successfully developed a methodology for assessment of this risk.

The incorporation of detect and avoid capability, including different sets of radar detection range and collision avoidance algorithms, making possible to decrease the NMAC rate by values ranging from 57% and 93%, applying the conditions assumptions assumed for this study in a realistic scenario with Intruders limited to 170 kt. [1].

A radar with 1 nm and $\pm 120^\circ$ of detection range, for instance, reduces 70% in NMAC rate when compared to flights without collision avoidance capabilities. This reduction by itself produces a safety level $2.247 \cdot 10^{-5}$ NMAC/hour for the Canadian average density. The NMAC rate reduction benefit when using longer range radars beyond 1 nm should be considered with respect to the safety improvements and costs of its implementation.

This tool allows future investigations of gains for investment/safety applying different levels of equipment for detect and avoid improvements for UAS.

The development and implementation of detection and avoidance systems for BVLOS operations of UAS, incorporating safety levels and best practice regulations set by TC and the Canadian NRC, enables the significant decrease in NMAC occurrences.

It was also determined, as a preliminary analysis, the implementation of the methodology to estimate the NMAC rates, and subsequently the risk, of the integrating UAS into the Canadian airspace.

As one specific application, it was demonstrated that surveillance operations on the Canadian Arctic can be performed with NMAC rates lower than the Canadian National Average without the utilization of radar or detect and avoid capability, being consequently a viable operation without the requirement of extra investment and development.

6.1 Future Work

Further analysis of specific operations for different traffic densities and patterns will include models with the simulation time beyond the current 60 seconds limitation from the model. The addition will make it possible to analyze the risk in a macro environment as well as specific scenarios already included in the developed application.

Currently maneuvers are limited to horizontal changes of heading, due to regulations and UAS limitations that impede the incorporation of UAS into the already widely implemented TCAS. Therefore, this thesis focused exclusively in horizontal DAA.

For future applications, 3D maneuvering, will also be conducted in order to estimate risk for applications in development for DAA equipment with different capabilities conforming to requirements established by MOPS. It is hoped that this work will be seminal for developing a

risk-based UAS regulatory policy in Canada, and may potentially influence similar policy-making by the FAA in the US and by internationally by ICAO.

Bibliography

- [1] RTCA, Inc, "Minimum Operational Performance Standards (MOPS) for Detect and Avoid (DAA) Systems," RTCA, 2017.
- [2] ICAO, "Unmanned Aircraft Systems (UAS)," International Civil Aviation Organization, 2011.
- [3] FAA, "Integration of Civil Unmanned Aircraft Systems (UAS) in the National Airspace System (NAS) Roadmap," 2013.
- [4] CASA, "Project OS 11/20 - Review of Regulations and Guidance Material relating to Unmanned Aircraft Systems (UAS)," [Online]. Available: <https://www.casa.gov.au/standard-page/project-os-1120-review-regulations-and-guidance-material-relating-unmanned-aircraft>.
- [5] R. Clothier, R. Walker, N. Fulton and D. Campbell, "A Casualty Risk Analysis for Unmanned Aircraft Systems (UAS) Operations over Inhabited Areas," *2nd Australasian Unmanned Air Vehicles Conference*, 2007.
- [6] EUROCONTROL, "EUROCONTROL Specifications for the use of Military Remotely Piloted Aircraft as Operational Air Traffic Outside Segregated Airspace," *European Organization for the Safety of Air Navigation*, no. First edition - 2013. U.S. Department of Transportation. Federal Aviation Administration, 2012.

- [7] K. H. J. Ruff-Stahl, S. Esser, D. Farsch, T. Graner and R. Klein, "Not-So-Risky Business? Assessing the Risk of Integrating Large RPVs into the Current Air Traffic System," *International Journal of Aviation, Aeronautics and Aerospace*, 2016.
- [8] P. Smith, "Roadmaps for Australian UAS Optimization," *AAUS Conference*, 2015.
- [9] CAA; Safety and Airspace Regulation Group, "Unmanned Aircraft System Operations in UK Airspace – Guidance," 2015, p. Cap. 722.
- [10] R. A. Walker and R. A. Clothier, "Safety Risk Management of Unmanned Aircraft Systems," in *Handbook of Unmanned Aerial Vehicles*, Springer, 2015.
- [11] M. Janic and F. Netjasov, "A Review of Research on Risk and Safety Modelling in Civil Aviation," *Journal of Air Transport Management*, pp. 213-220, 2008.
- [12] R. Melnyk, D. Schrage, V. Volovoian and H. Jimenez, "Sense and Avoid Requirements for Unmanned Aircraft Systems Using a Target Level of Safety Approach," *Risk Analysis*, p. 2014.
- [13] S. H. Stroeve, H. A. P. Blom and G. J. Bakker, "Systemic accident risk assessment in air traffic by Monte Carlo Simulation," *Safety Science*, p. 238–249, 2009.
- [14] D. W. King, A. Bertapelle and C. Moses, "UAV failure rate criteria for equivalent level of safety," Bell Helicopter Textron, 2005.

- [15] R. E. Weibel and R. J. Hansman, "Safety considerations for operation of Unmanned Aerial Vehicles in the national Airspace System," MIT International Center for Air Transportation, 2005.
- [16] European RPAS Steering Group, "Roadmap for the integration of civil Remotely-Piloted Aircraft Systems into the European Aviation System," 2013.
- [17] J. D. Stevenson, S. O'Young and L. Rolland, "Estimated levels of safety for small unmanned aerial vehicles and risk mitigation strategies," *NRC Research Press*, 2015.
- [18] C. Park, S. M. Lee and E. R. Mueller, "Investigating Detect-and-Avoid Surveillance Performance for Unmanned Aircraft Systems," in *14th AIAA Aviation Technology, Integration and Operations Conference*, 2014.
- [19] FAA, "Sense and Avoid (SAA) for Unmanned Aircraft Systems (UAS)," 2013.
- [20] S. X. Fang, Risk-based Supervisory Guidance Solutions for Detect and Avoid involving Small Unmanned Aircraft Systems, St. John's, 2017.
- [21] S. M. Lee, C. Park, M. A. Johnson and E. R. Mueller, "Investigating effects of well clear definitions on UAS sense-and-avoid- operations in enroute and transition airspace," in *Aviation Technology, Integration and Operations Conference*, 2013.
- [22] RTCA, "SC-147, Minimum Operational Performance Standards (MOPS) for Traffic Alert and Collision Avoidance System II (TCAS) Hybrid Surveillance," RTCA, Washington, 2006.

- [23] RTCA, "SC-228 Minimum Operational Performance Standards (MOPS) for Detect and Avoid (DAA) Systems," RTCA, Washington, 2017.
- [24] S. Baillie, W. Crowe, E. Edwards and K. Ellis, "Small Remotely Piloted Aircraft System (RPAS) Best Practices for BVLOS Operations," in *Unmanned Systems Canada Conference*, Edmonton, 2016.
- [25] A. D. Zeitlin, "Progress on Requirements and Standards for Sense & Avoid," MITRE, McLean, 2010.
- [26] D. Amarasinghe and S. O'Young, "Estimation of Alerting Thresholds for Sense-and-Avoid," in *IEEE International Workshop on Robotic and Sensor Environments (ROSE)*, 2010.
- [27] M. J. Kochenderfer, J. K. Kuchar, L. P. Espindle and J. D. Griffith, "Uncorrelated Encounter Model of the National Airspace System," Massachusetts Institute of Technology Lincoln Laboratory, Lexington, 2008.
- [28] M. J. Kochenderfer, L. P. Espindle, J. K. Kuchar and J. D. Griffith, "A Comprehensive Aircraft Encounter Model of the National Airspace System," *Lincoln Laboratory Journal*, 2008.
- [29] M. J. Kochenderfer, L. P. Espindle, J. K. Kuchar and J. D. Griffith, "A Bayesian Approach to Aircraft Encounter Modelling," in *AIAA Guidance, Navigation and Control Conference and Exhibit*, 2008.

- [30] A. Papoulis, *Probability, Random Variables, and Stochastic Processes*, New York: McGraw-Hill, 1984.
- [31] J. A. Jackson and J. D. Boskovic, "Application of Airspace Encounter Model for Prediction of Intruder Dynamics," in *AIAA Modelling and Simulation Technologies Conference*, 2012.
- [32] L. H. Sahawneh and R. W. Beard, "A Probabilistic Framework for Unmanned Aircraft Systems Collision Detection and Risk Estimation," in *53rd IEEE Conference on Decision and Control*, 2014.
- [33] R. E. Weibel, M. W. M. Edwards and C. S. Fernandes, "Establishing a Risk-Based Separation Standard for Unmanned Aircraft Self Separation," *Ninth USA/Europe Air Traffic Management Research & Development Seminar*, 2009.
- [34] K. Ellis, "Best Practices for small RPAS Beyond Visual Line of Sight," in *Unmanned Systems Canada Conference*, Edmonton, 2016.
- [35] Transport Safety Board of Canada, "Statistical Summary – Aviation Occurrences 2015," 04 2016. [Online]. Available: <http://www.bst-tsb.gc.ca/eng/stats/aviation/2015/ssea-ssao-2015.pdf>. [Accessed 10 05 2017].